



INSTITUT DE FRANCE
Académie des sciences

Comptes Rendus

Physique

Jérôme Weiss, Peng Zhang, Oğuz Umut Salman, Gang Liu and Lev Truskinovsky

Fluctuations in crystalline plasticity


Volume 22, issue S3 (2021), p. 163-199

<<https://doi.org/10.5802/crphys.51>>

Part of the Special Issue: Plasticity and Solid State Physics

Guest editors: Samuel Forest (Mines ParisTech, Université PSL, CNRS, France)
and David Rodney (Université Claude Bernard Lyon 1, France)

© Académie des sciences, Paris and the authors, 2021.
Some rights reserved.

 This article is licensed under the
CREATIVE COMMONS ATTRIBUTION 4.0 INTERNATIONAL LICENSE.
<http://creativecommons.org/licenses/by/4.0/>



*Les Comptes Rendus. Physique sont membres du
Centre Mersenne pour l'édition scientifique ouverte*
www.centre-mersenne.org



Plasticity and Solid State Physics / *Plasticité et Physique des Solides*

Fluctuations in crystalline plasticity

Fluctuations plastiques dans les matériaux cristallins

Jérôme Weiss^{*, a}, Peng Zhang^b, Oğuz Umut Salman^c, Gang Liu^b
and Lev Truskinovsky^d

^a ISTerre, CNRS/Université Grenoble-Alpes, 38041 Grenoble, France

^b State Key Laboratory for Mechanical Behavior of Materials, Xi'an Jiaotong University, Xi'an, 710049, China

^c CNRS, LSPM UPR3407, Sorbonne Université Paris Nord, 93430, Villetaneuse, France

^d PMMH, CNRS UMR 7636, ESPCI ParisTech, 10 Rue Vauquelin, 75005, Paris, France

E-mails: jerome.weiss@univ-grenoble-alpes.fr (J. Weiss), zhangpeng.mse@xjtu.edu.cn

(P. Zhang), umut.salman@lspm.cnrs.fr (O. U. Salman), lgsammer@xjtu.edu.cn

(G. Liu), lev.truskinovsky@espci.fr (L. Truskinovsky)

Abstract. Recently acoustic signature of dislocation avalanches in HCP materials was found to be long tailed in size and energy, suggesting critical dynamics. Moreover, the intermittent plastic response was found to be generic for micro- and nano-sized systems independently of their crystallographic symmetry. These rather remarkable discoveries are reviewed in this paper in the perspective of the recent studies performed in our group. We discuss the physical origin and the scaling properties of plastic fluctuations and address the nature of their dependence on crystalline symmetry, system size, and disorder content. A particular emphasis is placed on the formation of dislocation structures, and on our ability to temper plastic fluctuations by alloying. We also discuss the “smaller is wilder” size effect that culminates in a paradoxical crack-free brittle behavior of very small, initially dislocation free crystals. We argue that the implied transition between different rheological behaviors is regulated by the ratio of length scales $R = L/l$, where L is the system size and l is the internal length. We link this size effect with size dependence of strength (“smaller is stronger”) and the size-induced switch between different hardening mechanisms. We show that the task of taming the intermittency of plastic flow at ultra-small scales can be accomplished by generating tailored quenched disorder which allows one to control micro- and nano-forming and opens new perspectives in micro-metallurgy and structural engineering of miniature load-carrying elements. These insights were beyond the reach of conventional theoretical approaches that do not explicitly account for the stochastic nature of collective dislocation dynamics.

Résumé. Malgré une étude précurseur de Becker et Orowan en 1932 sur le Zinc, l'analyse des fluctuations dans la dynamique de la déformation plastique des matériaux cristallins a été pendant longtemps négligée, probablement du fait que dans la plupart des matériaux métalliques d'intérêt industriel ces fluctuations sont indétectables en termes de comportement mécanique aux échelles macroscopiques. La situation a changé drastiquement il y a une vingtaine d'années lorsque, d'une part, l'enregistrement des signatures acoustiques des avalanches de dislocations dans certains matériaux hexagonaux a montré que ces dernières pouvaient être distribuées en loi de puissance, suggérant une dynamique critique, et d'autre part il a été observé que la plasticité des systèmes de taille micro- et nano-métrique devenait intermittente pour la

* Corresponding author.

plupart des matériaux non-alliés. Dans cet article, nous discutons, sur la base de récents travaux et dans le cadre de la physique statistique, de la nature et des propriétés statistiques et d'échelle de ces fluctuations plastiques en fonction de la symétrie cristalline, de la taille du système considéré, ainsi que du désordre interne, qu'il soit émergent (structures de dislocations) ou ajusté par des techniques d'alliage. On met ainsi en lumière des effets de taille très prononcés sur la stochasticité de la déformation plastique, un rapport d'échelle $R = L/l$ entre la taille finie du système L et une échelle interne l jouant un rôle majeur pour expliquer ces transitions de comportement. On discute également le lien avec d'autres effets d'échelle, sur le seuil d'écoulement plastique ou la nature des mécanismes de durcissement, et on montre comment les techniques d'alliage peuvent réduire ces instabilités plastiques. Ceci ouvre la voie vers une métallurgie et des pratiques d'ingénierie aux échelles sous-microniques tenant compte du caractère stochastique intrinsèque de la plasticité à ces échelles, et tentant de le supprimer ou de l'atténuer.

Keywords. Plasticity, Dislocations, Statistical physics, Avalanches, Critical phenomena.

Mots-clés. Plasticité, Dislocations, Physique statistique, Avalanches, Phénomènes critiques.

Funding. The authors acknowledge the support of the French-Chinese ANR-NSFC grant SUMMIT (ANR-19-CE08-0010-01 and 51761135031). P.Z. acknowledges additional support from the China Scholarship Council and China Postdoctoral Science Foundation, grant 2019M653595.

Available online 26th March 2021

1. Introduction

Beyond the qualitative pioneering study of Becker and Orowan [1], the fluctuating nature of crystal plasticity has been largely overlooked for a long time, not in the least, because for most materials of engineering interest these fluctuations remained almost undetectable and considered as negligible comparing to the macroscopic response at bulk scales. The situation changed only when new technology opened a way to precision measurement of acoustic emissions accompanying plastic deformation. First, the acoustic signature of dislocation avalanches in HCP materials was found to be long tailed in size and energy, suggesting critical dynamics [2, 3]. Second, the intermittent plastic response was found to be generic for micro- and nano-sized systems independently of their crystallographic symmetry (e.g. [4, 5]).

1.1. *Continuum mechanics versus discrete approaches*

Following major discoveries during the “miraculous year” of 1934, lattice dislocations have been universally accepted as the main carriers of plastic deformation in crystalline solids [6–10]. The initially proposed dislocation theory was intrinsically discrete: plastic deformation was understood as resulting from the “quantized” activity of topological defects. An alternative concept of dislocations as singularities of continuum deformation fields has been developed much earlier and by that time was well established inside solid mechanics [11–13]. The singularity centered understanding of dislocations was not undermined by the new inherently discrete theory, for instance, the continuum theory of dislocations is still actively used in seismology [14]. However, it is by now universally accepted that none of these approaches is universal and that the type of description should depend on the scale of coarse-graining. In particular, it has been rigorously shown that the “quantized” lattice dislocations take the form of elastic singularities when the Burgers length scale is small comparing to length scales imposed by the loading [15, 16].

The subsequent progress in crystalline plasticity was based on the advances in our understanding of the structure of the cores of individual topological defects, in quantifying their short range interaction, and more recently in finding correlations in their collective dynamics. The continuum mechanical approaches to dislocation-driven plasticity were developed in parallel to lattice-based theories, starting from the pioneering works of Nye [17] and Kröner [18] who built the foundations of a field theory linking continuum displacement field to dislocation density tensor. For recent developments along these lines see [19–23].

Comparing to meso-scale modelling approaches, explicitly accounting for individual dislocations (or dislocation segments) and their interactions [24, 25], and to fully microscopic molecular dynamics simulations [26, 27], the conventional phenomenological continuum models of crystal plasticity offer the roughest description in the sense that they capture only the main effects of plastic yielding. They achieve the goal of representing complex geometries and loading conditions by drastically reducing the number of degrees of freedom. The implied spatial coarse-graining and temporal averaging is based on the identification of small internal length and time scales and relies on formal homogenization techniques allowing one to link the continuum variables with their lattice counterparts.

However, such a program has never been actually implemented rigorously in its full complexity and the existing continuum approaches to crystal plasticity remain largely phenomenological. Already the very idea of a pure continuum theory has several fundamental shortcomings. In particular:

(i) Identifying the appropriate internal length scale l remains an unsolved problem. In metals with multiple slip systems, such as FCC, it is known that dislocation patterns emerge spontaneously [28, 29]. These patterns may or may not be associated with a well-defined characteristic scale l_p [30]. In cases they do, l_p may represent a typical cell size or a spacing between persistent slip bands [31] and is generally of the order of a few μm in FCC materials. It would then be inversely proportional to the yield stress due to the similitude relation (see more below) [25, 32]. When such a scale can be unambiguously defined, it may be tempting to identify the homogenization scale l with l_p . With all this said, the determination of l_p , as well as the check of the correctness of the similitude relation, remain fully empirical. Moreover, in crystalline structures characterized by a strong plastic anisotropy, such as HCP crystals, the implied dislocation patterns with a well-defined characteristic size do not form at all [33], which leaves the question of the averaging scale completely open.

(ii) There has been an increasing evidence of the existence of temporal fluctuations in crystalline plasticity induced by cooperative motions of dislocations. The intermittent dynamics was qualitatively recognized in HCP crystals long ago [1], however, it has not been analyzed quantitatively till the turn of this century [2, 3]. This became a bigger issue when it was realized that, upon decreasing the system size below few μm —noticeably, the same order of magnitude as the characteristic scale l_p —, plastic deformation becomes jerky independently of crystal symmetry [4, 34, 35]. It raised major concerns regarding manufacturing and reliable utilization of ultra-small machinery [36, 37]. By construction, the phenomenological continuum models and field theories are unable to deal with such fluctuations, unless stochastic closures are implemented implicitly [38, 39].

(iii) By construction, the continuum dislocation density tensor only accounts for dislocations generating a net plastic distortion at a given scale l , the so-called “geometrically necessary dislocations (GND)”. It, therefore, ignores the “statistically stored” dislocations (SSD) with zero net Burgers vector [13]. This is a strong limitation as SSD are tightly linked to hardening. In principle, this problem can be “resolved” through a decomposition of the dislocation density tensor into contributions from different slip systems combined with a very high spatial resolution, well below the average dislocation mean-free path [40]. At that resolution any dislocation becomes geometrically necessary, however, it would completely eliminate the advantage of a continuum description [41]. Instead, the continuum descriptions fully focused on the internal elastic fields associated with GND can hardly deal with dislocation nucleation and other processes involving short-range interactions such as multiplication, annihilation, or the formation of junctions. There are, however, recent developments in this direction that are promising [41].

Some macroscopic plastic instabilities and jerky plastic flows in alloys have been linked to dynamic strain aging related to the diffusion of solutes towards dislocation cores and the unpinning

of dislocations from these point defects [42–44]. This interesting but somewhat specific problem has been thoroughly analyzed elsewhere, often from an augmented continuum framework without reference to lattice dislocations [45]. We leave it outside the scope of the present paper focusing on pure crystals, or systems containing passive quenched disorder. In such systems, intermittent fluctuations have a completely different origin and remained so far beyond reach for continuum theories.

It has to be also mentioned that unlike elasticity, plasticity is a dissipative process generating heat and producing irreversible deformations. This implies that a purely mechanical description in terms of interacting purely elastic defects, either discrete or continuous, is inadequate, and argues instead for a thermodynamical approach [46]. However, it is immediately clear that weakly nonequilibrium thermodynamics, which has been successful in describing linear viscoelasticity and heat conduction, would not be sufficient because plasticity involves threshold type nonlinearity and is therefore non linearizable. Even though the fully adequate, strongly nonequilibrium statistical mechanics has not been developed yet, the attempts to model plasticity directly in statistical mechanics terms by viewing crystal as an ensemble of interacting, out of equilibrium defects has been made repeatedly since the early days of dislocation theory, see the review in [47].

The elusive character of the initial hopes to use equilibrium statistical mechanics was however soon realized. If point interactions within a gas are weak, dislocations, represented by line segments, interact strongly both at short-range (direct entanglements and depinning) and at long range (transmitted by elastic fields). The combination of threshold type interaction and the extended nature of the interacting defects gives rise in a driven system to a rich repertoire of dynamic behaviors characterized by cooperative effects and self-organization. The emerging scaling laws are thus just a signature of the underlying highly correlated collective dynamics. Moreover, dislocations are defects with an energy much higher than the energy of thermal fluctuations, which can hardly affect them. Therefore, a driven system undergoing plastic deformation remains at room temperature far from thermal equilibrium [25]. Instead of thermalization, complex metastable out-of-equilibrium dislocation patterns emerge and intermittently store and dissipate the energy constantly delivered by the loading device. One can say that the energy effectively flows through the system, arriving at macro scale and dissipating at the scale of dislocation cores. The emerging downscale energy cascade is probably as complex as in the case of turbulent flows with power law scaling similarly emerging in the intermediate “inertial” range.

Despite these impediments, there have been recent attempts to build a thermodynamic theory of crystalline plasticity by assuming only partial thermalization involving large but limited number of degrees of freedom. Such approaches have been successful in rationalizing some of the phenomenology of dislocation patterning and came up with an original understanding of strain-hardening which relies on first principles type arguments [47–49]. Theories of this type were particularly effective in dealing with elevated temperatures and nonzero loading rates in crystals with significantly inhibited long range dislocation interactions. In such systems, the role of elasticity is weak, and the correlations resulting from self-organization of defects are suppressed. This allows for at least partial thermodynamic equilibrium to be achieved. Despite these successes, it is probably safe to say that a broadly applicable thermodynamic theory of plasticity has not been yet developed.

1.2. *The goals of this review*

Our aim here is to discuss in some detail recent advances in the characterization and modelling of plastic fluctuations in space, time and energy domains. We discuss why plastic flow in crystals often occur through intermittent slip avalanches that are power-law distributed and in this sense scale-free [2, 3]. While the presence of such highly correlated fluctuations clearly

suggests the *critical* character of collective dislocation dynamics, the nature of the underlying self-organization mechanism is still highly debated [5, 50, 51]. The literature devoted to plastic intermittency, dislocation avalanches, and the associated criticality is steadily growing and an exhaustive review of the subject is far beyond the scope of this paper. The early work was reviewed in [52] and more recent comprehensive discussions can be found in [53–61]. The goal of this review is to address only the subjects in whose development some of us have played an active role.

As we have already mentioned, the discussion will be centered around the physical origin of the scaling behavior. Along the way, we will also address the nature of the dependence of the critical exponents on crystalline symmetry, system size, and disorder content. We only touch upon such important emergent behaviors as the formation of dislocation structures and system size events.

The recent discovery that the reported scaling in crystal plasticity is not universal, and that the measured power law scaling exponents depend on lattice structure, crystal orientation in the loading machine, the size of the crystal, its purity, and the presence or the absence of hardening [33, 62–64, 64–66], reveal rich and complex physics of the underlying self-organization process that still remains largely unexplored [67]. Without attempting to make a comprehensive exploration of the elemental plasticity mechanisms, we concentrate on the recent work addressing: (i) experimental tracking of plastic fluctuations either directly from stress–strain records [64, 68], or from acoustic emission (AE) in bulk materials [62, 66, 69]; (ii) numerical simulations based on the minimal automaton model of plastic flow in crystals proposed in [67, 70]; (iii) stochastic modeling of mesoscale crystal plasticity introducing rheological closure relations with multiplicative noise [62]. Our various comments on the recent progress in the field are therefore highly biased by our own experimental and computational work and are presented in the perspective of the studies performed in our group.

We begin by summarizing the current understanding of the nature of scaling in pure materials. In particular we raise the question why and how the associated exponents depend on crystal symmetry and system size. We then explain how the transition from mild (Gaussian-like) to wild (power law distributed) fluctuations is controlled by an internal length scale l and use the obtained understanding to build a connection with plastic hardening. Our next subject is the “smaller is wilder” size effect that culminates in a paradoxical crack-free brittle behavior of very small, initially dislocation-free crystals. We show that the implied transition between ductile and brittle rheological behaviors is regulated by the ratio of length scales $R = L/l$, where L is the system size. We link this relatively new size effect with some other well-studied phenomena like the size dependence of strength (“smaller is stronger”) and the size-induced transition between different hardening mechanisms.

After gaining an insight regarding plastic fluctuations in pure crystals, we broaden the scope of our discussion to include alloys, and show that, in submicron samples, altering the alloying-induced quenched disorder may serve as a proxy for the variation of the system size. We show that the transitions in the statistical structure of these fluctuations induced by the ratio between the external size and a disorder-dependent internal scale can be rationalized within a simple numerical model allowing to obtain quantitative relations between the system size and the scaling exponents.

We then turn to one of the main technological challenges in nanoscience which is to tame the intermittency of plastic flows at sub-micron scales. We show that this task can be accomplished by introducing tailored quenched disorder, i.e. from alloying, which allows one to control micro- and nano-scale forming. This understanding opens new perspectives in nanometallurgy aiming not only at improving mean properties (e.g. strength) but also at tempering associated deleterious variability of the response.

To conclude, we reiterate that the problems posed by the emerging science of structural engineering of sub-micron load-carrying elements cannot be solved by using conventional methods of continuum plasticity and equilibrium statistical mechanics. New methods are needed, taking explicitly into account the out of equilibrium, highly correlated nature of collective dislocation dynamics. These methods are only now being developed and our review should be viewed as a step in the direction of clarifying and sharpening some of the most important underlying questions.

2. Pure materials

2.1. Historical background

The first reported evidence of intermittent plasticity dates back to the pioneering study of Becker and Orowan, who observed during the deformation of Zinc crystal rods a succession of sudden strain jumps of vastly different sizes [1]. It is worth stressing that these experimental results likely played a substantial role in elaborating dislocation theory by Orowan two years later [6, 56]. Forty years after Becker and Orowan, plastic bursts were observed again in Zinc crystals, still directly on stress-strain curves [71]. As we are going to explain below, it is not incidental that all these initial observations of jerky plastic flow were made on HCP crystals characterized by a strong plastic anisotropy.

Outside these pioneering observations, the intermittency of plastic deformation was only episodically addressed until the late 90's. In classical continuum theory, it was implicitly assumed that the inevitable fluctuations resulting from discrete dislocation motions average out and become invisible at engineering scales. These fluctuations were believed to be associated with a particular mesoscopic scale that is much smaller than the scale of the observations. They were also perceived as roughly Gaussian or *mild* in the terminology of Mandelbrot.

However, experimental investigations of plastic fluctuations continued to challenge this picture. In the late 60's, a new generation of experiments was performed using indirect monitoring tools which switched attention from stress-strain curves to acoustic emission (AE) accompanying plastic flow. Several authors reported acoustic bursts during plastic deformation in materials with different crystal symmetries, and interpreted them as a signature of slip events resulting from cooperative dislocation motions [72, 73]. In FCC metals, such burst-like AE activity was scarce, with maximum intensity at plastic yield but fading away rapidly as the material strain-hardened. It was also superimposed on the so-called continuous AE [74, 75]. This slow evolving background “noise” was interpreted as resulting from the cumulative effect of numerous, small and *uncorrelated* dislocation motions, in full contrast with the cooperative motions giving rise to discrete AE bursts. The AE source model that was used to link the characteristics of the recorded AE signals to local dislocation motions is detailed elsewhere [62, 76]. Very generally, this model assumes that for discrete AE signal, the radiated acoustic energy E_{AE} integrated over the waveform duration is proportional to the mechanical energy dissipated by the plastic event at the source. For continuous AE, the acoustic power dE_{AE}/dt is taken as a proxy of the plastic strain-rate.

Now, nearly 50 years after these historical studies, it is rather striking to discover how many modern issues related to plastic fluctuations have been already implicitly identified at that time. Those include the role of crystal symmetry, the influence of strain hardening, and the possible coexistence of large cooperative motions (dislocation avalanches) with small uncorrelated motions. However, these early studies neither provided the quantitative analysis of fluctuations nor did they offer a framework for the interpretation of the observed intermittency.

A few decades later, the whole subject was reactivated when AE was finally carefully recorded during the plastic deformation of ice single crystals, and the obtained time series were statistically

post-processed [2, 3]. Subjected to uniaxial compression, this HCP material with a particularly strong plastic anisotropy [77], unexpectedly revealed a fully intermittent AE signal characterized by a succession of bursts that were power-law distributed in energies. The obtained data could be fit using a relation for the probability density $P(E_{\text{AE}}) \sim E_{\text{AE}}^{-\kappa_E}$. The value of the exponent κ_E was found to be somewhat close to the mean-field value 1.5 [5, 78, 79] and independent of either the applied stress or the temperature [2, 3].

Using the same material, it was further shown that the dislocation avalanches are clustered in time. More precisely, it was demonstrated that the larger the energy of an avalanche, the larger, in average, is the avalanche occurrence frequency immediately after that avalanche. These observations were interpreted as an evidence of “aftershocks” triggered by the main stress redistribution [80]. Spatial clustering, i.e. a fractal structure of avalanche distribution, was detected as well. Moreover, spatial and temporal distributions of avalanches were found to be linked. More precisely, aftershocks turned out to be triggered in the vicinity of their “mainshock”, which is a consequence of stress transfer decay with the distance from the mother avalanche [81]. All these observations were later confirmed on other HCP materials such as Zinc or Cadmium, with the exponent κ_E taking values close to that observed for ice [82].

The obtained results argue that in HCP crystals the collective dynamics of dislocations self-organizes towards criticality. Consistently with earlier observations of jerky stress-strain curves [1, 71], plastic deformation in such materials takes the form of well-separated avalanches. The statistics of these avalanches was found to be of power-law type and their maximum size was constrained only by the size of the system. In Mandelbrot’s terms this means that the fluctuations are *wild* suggesting that quasi-statically driven HCP crystals are inherently critical.

Intermittent, power-law distributed plastic fluctuations were also identified from both AE measurements and high-resolution extensometry in a FCC material, copper, at least in the early stages of deformation [83]. However, compared to avalanches in HCP materials, the detected plastic bursts in copper were much more sporadic, which confirmed observations made in earlier studies [74, 75]. The scarcity of avalanches could not be truly quantified at that time and its conceptual importance was understood only recently [62], see more about this below. Aftershock triggering, signing interactions between avalanches, is however also observed in FCC materials [84].

Overall, the AE measurements in both HCP and FCC crystals appear to be arguing for a scale-free, critical character of crystalline plasticity. We recall that this is at odds with the classical paradigm of dislocation-mediated plasticity as a smooth flow resulting from small, uncorrelated and fundamentally similar increments and that was also the picture emerging from the observations on bulk BCC materials. All this naturally raises the question whether these two conflicting pictures can be reconciled. A related question is whether the critical nature of crystalline plasticity, at least in HCP and FCC crystals, is universal and is characterized by a set of critical exponents that are independent of the particular material and its purity, of the size and shape of the sample and of the loading conditions.

In what follows, we try to answer these questions addressing separately the role of crystal symmetry, the system size L and the quenched microstructural disorder. We will not address the role of grain boundaries (GB) because this question has received so far only very limited attention. There are, however, experimental and numerical studies showing that GBs can hinder the development of dislocation avalanches, although a spatially correlated plastic activity can spread in polycrystals over much larger distances [33, 85–87]. In other words, we consider single crystals only, ranging from \sim cm to \sim nm external sizes, but do not address the role of grain size on strength [88] or plastic intermittency [89] in nanocrystalline polycrystals.

2.2. From subcritical to supercritical plasticity

Over the last years, the growing interest towards manufacturing devices at micro- to nano-scales challenged the classical, size-independent approaches of material engineering and called for new approaches to mechanical characterization of materials at such small sizes [52, 54]. Compression tests from a flatbed indenter on μm to sub- μm pillars became a standard tool for such characterization [4, 53, 90]. Other methodologies have been proposed to explore even smaller (few tens of nm) systems, such as tensile tests on nanowires [91] or compression of nanoparticles [92, 93].

The first outcome of these studies was a discovery of a dramatic size effect on strength τ_y which is usually defined as the shear stress reached at some arbitrarily specified amount of plastic deformation [90]. This “smaller is stronger” phenomenon is usually expressed through a scaling $\tau_y \sim L^{-\alpha}$, with α an empirical exponent varying for metals in the range 0.2–1 [54, 94, 95]. The conventional interpretation of this size effect is the increased role of free surfaces in small systems. The associated mechanisms are known as source truncation [96] or dislocation starvation [97]. In initially dislocation-free nanoparticles, yield stresses close to the theoretical shear strength have been reported and linked to a size-specific particular dislocation nucleation mechanism [92].

Besides the size effect on strength, compression tests on micropillars of FCC [4] and BCC materials [34, 98] revealed stress–strain curves with an anomalous presence of intermittent strain bursts. These bursts were shown to be power-law distributed with the probability distribution $P(s) \sim s^{-\kappa}$ where s is the burst size.

This observation was in contrast with the scarcity of such plastic bursts at bulk scales, and the association of these materials with a smooth macroscopic response, a dominance of multi-slip and a presence of a single scale in dislocation patterning. It suggests that there is a distinct fluctuation-related size effect which was coined as “smaller is wilder” [62]. A wealth of experimental work confirms the emergence of intermittent plastic bursts in sufficiently small crystals of both pure materials and alloys. The ubiquity of power-law distributed plastic bursts at small L triggered an intense debate regarding the physical nature of this phenomenon [5, 50, 63, 99].

In this section we consider pure materials with different crystalline structures with the goal of exhibiting the rich landscape of plastic fluctuations and showing how it evolves with the system size. The effect of extrinsic disorder (alloying) will be studied in following sections.

Figure 1 shows experimental results: in (a) the true stress–true strain relations, and in (b) the cumulative distributions of displacement burst sizes X (in nm). In (c) we illustrate the deformation morphology for compression tests for μm to sub- μm pillars of a high-purity BCC material, Mo [67]. In these experiments, the loading configuration was designed to ensure that twinning was absent, i.e. plasticity was accommodated by dislocations only. A size effect on the yield stress is apparent on Figure 1(a). The plastic displacement jumps along the compression axis were extracted from the force-displacement raw data using a methodology detailed in [64]. An avalanche was defined as a plastic process characterized by a dissipation rate much greater than the imposed loading rate. The size s of the dislocation avalanche can be linked to the plastic jump X , which is assumed to scale with the cumulative distance covered by all mobile dislocations during the avalanche [100]. The distributions presented on Figure 1(b) contain results from at least four samples of the same size L .

Figure 1(b) illustrates the “smaller is wilder” size effect. For the larger pillars ($L = 1500$ nm), the relatively smooth mechanical response (Figure 1(a)) produces a distribution of plastic fluctuations which clearly has nothing to do with power law, instead revealing a characteristic size X_0 (see more below) and corresponding to a *sub-critical* regime. At an intermediate sample size $L = 1000$ nm, the nature of plastic fluctuations changes drastically, with a power law distribution

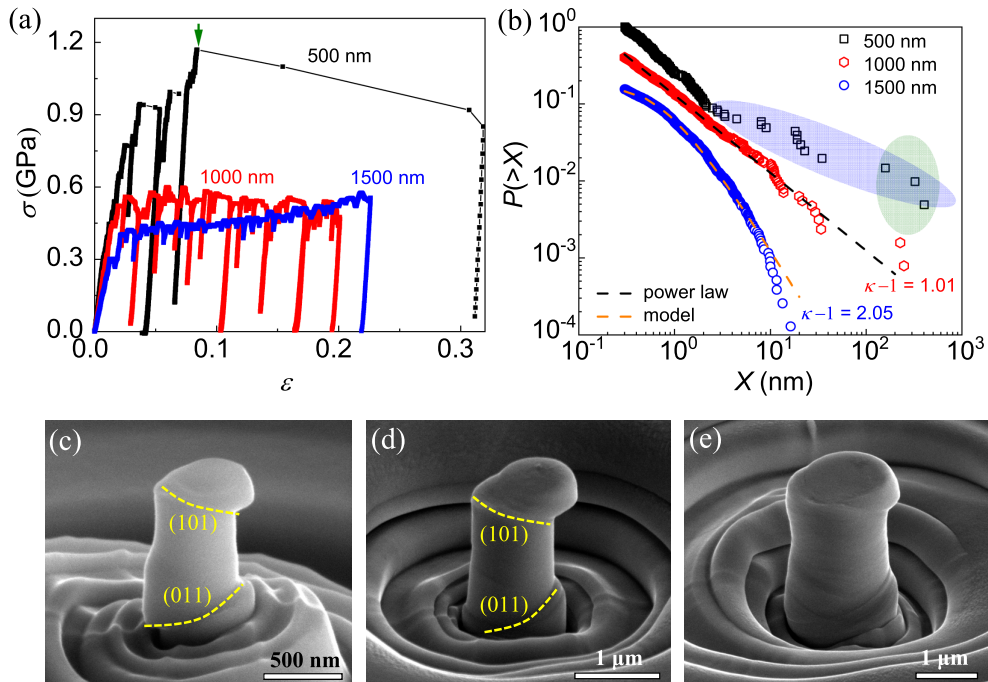


Figure 1. From mild to supercritical fluctuations in Mo micropillars. (a) Stress–strain curves (shear). (b) Cumulative distributions of plastic displacements X detected over the entire loading. The events marked in violet correspond to supercritical events, while those marked in green are dragon-kings, system-spanning events. Dashed line represent the fits of the data with (2). (c)–(e) SEM images of (c) 500 nm, (d) 1000 nm and (e) 1500 nm [112]-oriented micropillars after compression. The marked slip traces indicate the locally single-slip nature of the plastic flow in 500 nm and 1000 nm pillars. Adapted with permission from [67]. Copyrighted by American Physical Society.

of avalanche sizes, $P(>X) \sim X^{-(\kappa-1)}$ emerging over three orders of magnitude, without detectable lower or upper cut-offs, and with $\kappa \approx 2.0$. A robust maximum likelihood methodology has been used in all our analyses to estimate such exponents as well as to detect possible lower or upper cut-offs [101]. The power law statistics in this range of crystal sizes characterizes a scale-free, critical dynamics, reminiscent of what was observed in several other studies (e.g. [3, 5, 52]).

As we decrease further the system size to 500 nm, the nature of plastic fluctuations changes again, producing a regime characterized by the presence of large scale outliers coexisting with a power-law range at small scales. The appearance of “dragon-kings” can be interpreted as a transition towards a *supercritical* dynamics [102]. The largest of the outliers correspond to system-spanning avalanches resulting in a global “failure” of the pillar; one such system size avalanche is marked by an arrow on Figure 1(a). Note that the corresponding mechanical response is brittle-like, with only few inelastic events preceding the major collapse. This is similar to the previously studied behavior of compressed nanoparticles in the diameter range 200–800 nm. They show an extreme case of brittleness with a unique system-spanning dislocation avalanche preceded by a purely elastic response [92, 103]. However, a quantitative comparison of our BCC pillars (Mo), fabricated from a bulk sample containing pre-existing dislocations, and such FCC (Au and Ni) nanoparticles, fabricated from solid-state dewetting and initially dislocation-free, has to be done with caution.

All these observations argue for a rich spectrum of mechanical behaviors depending on the crystal size L : from a smooth, ductile-like response associated with non-scale-free (mild) fluctuations in “large” crystals, to a purely brittle behavior characterized by a single dragon-king event in “small” crystals. In this context, the critical scale-free dynamics, observed in our Mo pillars for $L = 1000$ nm, appears as an intermediate regime underlying a brittle-to-ductile (BD) transition which can be then associated with a particular range of system sizes.

Interestingly, a brittle-to-ductile (BD) transition is usually discussed in the context of fracture, with dislocation nucleation at crack tip indicating the emergence of ductility [104, 105]. The results presented above argue for a BD transition “without a crack”, i.e. in terms of collective behavior of dislocations characterized by a particular scale-free structure of plastic fluctuations. In this case, rather paradoxically, the nucleation of individual dislocations is associated with a brittle regime [93].

2.3. The concept of wildness

In the setting discussed above, the evolution from super- to sub-criticality over a range of system sizes occurs in a BCC material. In fact, a similar dependence of the plastic fluctuations on system size L has been also observed in FCC materials. As already noted, initially dislocation-free FCC nanoparticles do exhibit brittleness, even though a supercritical regime has not (yet) been observed for FIB-fabricated FCC pillars. The latter may be related to the difficulty of fabricating dislocation-free crystals due to the easiness for Ga^+ ions to penetrate light FCC crystals, which generates FIB-induced defects (small dislocation loops) near the surface [106, 107].

However, a recent study [108] showed that such FIB-induced dislocation loops in Al micropillars can be eliminated by thermal annealing, which makes the stress-strain response more brittle-like. Unfortunately, the associated statistics of strain burst sizes has not been analysed. While our observations on BCC crystals argue for a sharp transition from a critical dynamics at $L \sim \mu\text{m}$ to a more ductile behavior at larger system sizes [34, 64], similar transition seems to be more gradual for FCC materials. Figure 2 illustrates this effect for pure Al. While the size effect on strength is still apparent (Figure 2(a)), slip burst distributions are characterized by a power law tail over a wider L -range (~ 500 – 3500 nm) than for Mo, with $\kappa \approx 1.6$ – 1.7 , closer to the mean-field value 1.5 (Figure 2(b)). At larger system sizes, say $L = 6 \mu\text{m}$, a larger exponent emerges, in association with a smoother mechanical response. These observations may be viewed as another argument supporting the idea of non-universal character of the exponent κ .

One can show that all the distributions shown in Figure 2(b) are well described by the generic formula

$$P(X) = \frac{X_0^{\kappa-1}}{\Gamma(\kappa-1)X^\kappa} e^{-X_0/X} \quad (1)$$

$$P(> X) = 1 - \frac{\Gamma\left(\kappa-1, \frac{X_0}{X}\right)}{\Gamma(\kappa-1)}, \quad (2)$$

where $\Gamma(a, x)$ is the incomplete gamma function, and the exponential term represents a *lower* cut-off to power law statistics occurring around $X = X_0$. These expressions characterize the presence of wild (scale free, power-law distributed) fluctuations at large scales $X \gg X_0$, coexisting with mild fluctuations associated with a characteristic size X_0 at small scales. Equations (1)–(2) received a theoretical support from a simple mean-field stochastic model of dislocation dynamics [62], which we will discuss in some detail later in the paper (see Section 5.2).

Note that for pillar sizes $L \geq 1 \mu\text{m}$, see Figure 2(b), the lower cut-off X_0 is not an experimentally imposed threshold. In particular, it increases for the largest Al pillars. This will become even more apparent when we consider alloys (see Section 3). However, it is clear that a large range of mild

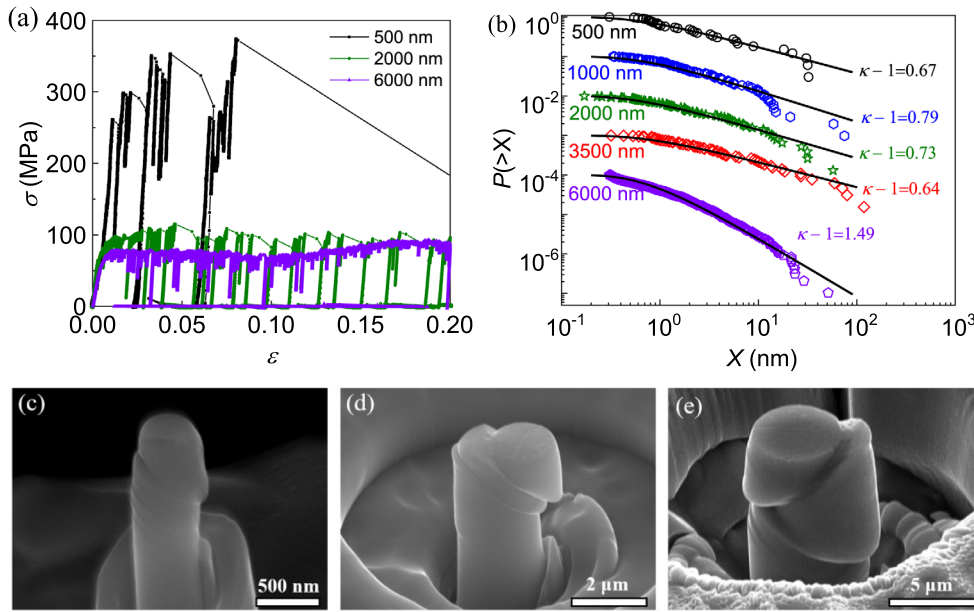


Figure 2. From mild to wild fluctuations in Al micropillars. (a) Stress–strain curves (shear). (b) Cumulative distributions of plastic displacements X detected over the entire loading. The solid lines represent the fit of the data with (2), and the corresponding lower cut-off values X_0 are, from top to bottom: 0.64, 0.73, 0.61 and 1.02 nm. (c)–(e) SEM images of (c) 500 nm, (d) 2000 nm and (e) 6000 nm micropillars after compression. Multislip is only observed for the largest micropillars (6 μ m). Adapted with permission from [64].

fluctuations, with sizes $X < X_0$, remain undetected by our methodology [64]. This is particularly the case for $L = 500$ nm Al pillars and $L = 1$ μ m Mo pillars, where the lower cut-off is hardly discernible on our data.

In addition, we did not find any statistical evidence of an *upper* cut-off limiting the power law range in our Al data, independently of L . In particular, for the 1500 nm Mo pillars (Figure 1(b)), Equation (2) with a large κ value fits well the data. In that case, however, the generic form given above can be hardly differentiated from a log-normal distribution. In any case, all this means that the observed sub-critical regime is strongly dominated by mild fluctuations.

The relative contribution of mild versus wild fluctuations to the total plastic strain can be reasonably estimated. We call X_{\min} , the value, close to X_0 , above which fluctuations can be considered as being power-law distributed, i.e. wild, and write $K = e^{-X_0/X_{\min}}$. Then, the probabilistic weight of the wild part of the distribution (1), measuring the amount of plastic strain accommodated through scale-free avalanches, which we call *wildness*, and denote by W , can be written as (see also Section 5.2) [62]:

$$W(\kappa, K) = 1 - \frac{\Gamma(\kappa - 1, \ln(1/K))}{\Gamma(\kappa - 1)}. \quad (3)$$

The most striking point here is the link between the wildness W and the power law exponent κ , with large W being associated with smaller values of exponents. Experimentally, κ as well as the lower bound X_{\min} can be estimated using the maximum-likelihood methodology [64, 101], and X_0 found from a best-fit of (2). The plastic strain dissipated through scale-free avalanches can be independently calculated by accumulating all the strain bursts above X_{\min} , then comparing the associated strain to the total plastic strain in order to estimate W [64]. We will show later in

Section 3 that (3) is consistent with experimental data for a surprisingly broad range of materials, including pure metals and alloys.

Here we only mention that FCC materials are characterized by an extended BD transition taking place with increasing system size. A new finding is that this transition is associated with a progressive evolution of wildness and exponent κ . We recall that in such bulk materials macroscopic plasticity is mostly smooth (“ductile”) with only scarce bursts detected by AE (see Section 2.1). At the macroscopic scales a proxy of wildness can be estimated from W_{AE} , by summing the energies of the detected bursts and comparing with the total emitted acoustic energy (both continuous and discrete, see Section 2.1) [33,62]. In bulk FCC materials, W_{AE} rapidly decreases to a few % or less as strain hardening takes place and a dislocation substructure forms [62, 69]. This is particularly visible under cyclic loading where dislocation avalanches become exceptionally rare already after few cycles [66] (see Section 4).

Despite the achieved understanding, the issue remains with BCC materials exhibiting a sharper BD transition than FCC materials. The origin of this difference will be discussed in the next section.

2.4. External versus internal length scales

The results presented above show clear evidence of the strong effect of the system size on plastic fluctuations. The quantitative role of such an external scale can be studied if we present it as a ratio of two length scales, $R = L/l$, where l represents some judiciously chosen internal length scale. The resulting nondimensional parameter will then control the collective dislocation dynamics [64].

In case of the Mo pillar experiments illustrated in Figure 1, the initial dislocation density before loading was measured giving $\rho = 1.6 \times 10^{12} \text{ m}^{-2}$. This implies that the mean dislocation spacing is $l_d = 1/\sqrt{\rho} \approx 790 \text{ nm}$. We can interpret the length l_d , which is naturally present in all pure materials, as an internal scale.

With this interpretation at hand, we note that supercriticality is observed for $L < l_d$ meaning $R < 1$ and subcriticality for $L > l_d$ or $R > 1$. This is not incidental, and illustrates the role of the mutual interactions between dislocations (short-range and long-range) in setting the internal dynamics.

Indeed, for $R < 1$, preexisting (and mostly locked) dislocations, serving as potential obstacles in ensuing dislocation dynamics, are almost absent. Therefore the work of the loading device is dissipated through a collective nucleation and correlated motion of unlocked dislocations. In particular, such lack of inhibition leads to the emergence of super-critical instabilities.

Instead, for $R \gg 1$, moving dislocations necessarily encounter a considerable number of different obstacles, in particular, forest dislocations. In this context, cross-slip as well as short-range interactions are promoted, frustrating the development of system-size correlated dislocation avalanches. Hence, mild fluctuations and a ductile-like behavior ensue. In BCC materials large lattice friction will likely play a role as well in inhibiting large avalanches (see more on this below).

Over an intermediate range, $R \sim 1$, i.e. for $L \sim l_d$, we observe that while the pillars are not initially dislocation-free, short and long-ranged (elastic) interactions are nicely balanced, which apparently creates the right environment for self-organization to a scale-free, critical avalanche dynamics. The deformation morphologies shown on Figure 1(c)–(e) support this interpretation: at small pillar sizes, plastic deformation is highly anisotropic with a clear domination of a single slip plane, while at large pillar sizes, the plastic flow is more diffuse and isotropic as the result of the dominating multislip deformation.

A natural way to define the internal length scale l in the general case is to write [25, 64, 109]:

$$l = Gb/\tau_{\text{pin}}, \quad (4)$$

where G is the shear modulus and b the Burgers's vector. The new parameter τ_{pin} is the effective pinning strength of the existing obstacles inhibiting dislocation motion. We can write

$$\tau_{\text{pin}} = \tau_l + \tau_f + (\tau_s + \tau_p), \quad (5)$$

where τ_l is the lattice friction, $\tau_f = \alpha_f Gb\sqrt{\rho_f}$ is the pinning strength of forest dislocations (with constant $\alpha_f < 1$). The two other terms, τ_s and τ_p , corresponding to extrinsic disorder and describing the effects of solutes and precipitates, respectively, will be discussed in Section 3 devoted to alloys. Given this definition, the internal scale l corresponds to the distance at which the dislocation/dislocation elastic interaction stress (scaling as Gb/l) becomes comparable to the dislocation/obstacle interaction stress τ_{pin} .

Experimentally, τ_{pin} can be in principle obtained from the yield strength under tension of bulk samples [64]. However, caution is necessary when we deal with small scales. Consider e.g. BCC materials below an athermal transition temperature T_a . Then the lattice friction experienced by screw dislocations is large as the result of their compact core structure [110]. This implies the necessity to overcome large barriers through thermal activation. Our tests on Mo, performed at room temperature, belong to this range, as $T_a \approx 465$ K in this material [25]. In FCC materials, where lattice friction is small, independently of the temperature, one can expect a smaller value of τ_l than in the case of BCC. This would lead to a larger value of the internal scale l and will increase the L -range over which large fluctuations are expected. To confirm this conjecture we compare in Figure 3 the data for Mo (BCC), Al (FCC) and Mg (HCP) pillars of the same size (3500 nm). In particular, the Mo pillars display a much smoother mechanical response and a larger exponent $\kappa \approx 4.0$. Given this scenario, one would expect the difference between FCC and BCC to disappear for $T > T_a$, when the role of thermal activation in the dynamics of screw dislocation disappears. This assertion is supported by the results reported in Abad *et al.* [111], where stronger plastic intermittency in BCC materials at higher temperatures was observed. At these temperatures lattice friction apparently no longer inhibits large scale self-organization and the nature of the internal scale l changes.

Another factor biasing the competition between short-range and long-range interactions is the damping of dislocation motion: if strong enough, it can inhibit fast dislocation avalanches [112]. Consistently with this observation, plastic intermittency is suppressed in micropillars deformed at strain-rates ($\geq 1 \text{ s}^{-1}$) that are larger than the internal relaxation rate limited by lattice friction [113]. The damping related effects should not, however, depend on the system size L , which excludes its role in the critical to super-critical transition observed in BCC micropillars even at low T (Figure 1). Here it is appropriate to refer to recent DDD simulations which suggest that at low $T < T_a$ and relatively large system sizes, strain fluctuations are controlled by the slow (thermally activated) screw dislocation motion, hence avalanches can be damped [112]. Instead, at sub- μm sizes, the external stress imposed on samples enhance the athermal mobility of screw dislocations to the level of edge dislocations, making irrelevant the thermally activated motion. In particular, the DDD simulations show a reduced sensitivity of strength to temperature as the size of BCC micropillars diminishes [114]. This implies that the damping mentioned above is suppressed, which allows the initiation and propagation of strain bursts [112]. To summarise, switching from long- to short-ranged interactions and variable role of damping may be the factors explaining the sharper BD transition observed in BCC compared to FCC metals.

Questions, of course, remain regarding the interpretation of the internal scale l as defined by (4). In BCC materials, dislocation patterning and cell formation are not observed below a certain value of applied strain, which strongly increases with decreasing temperature. This is related to

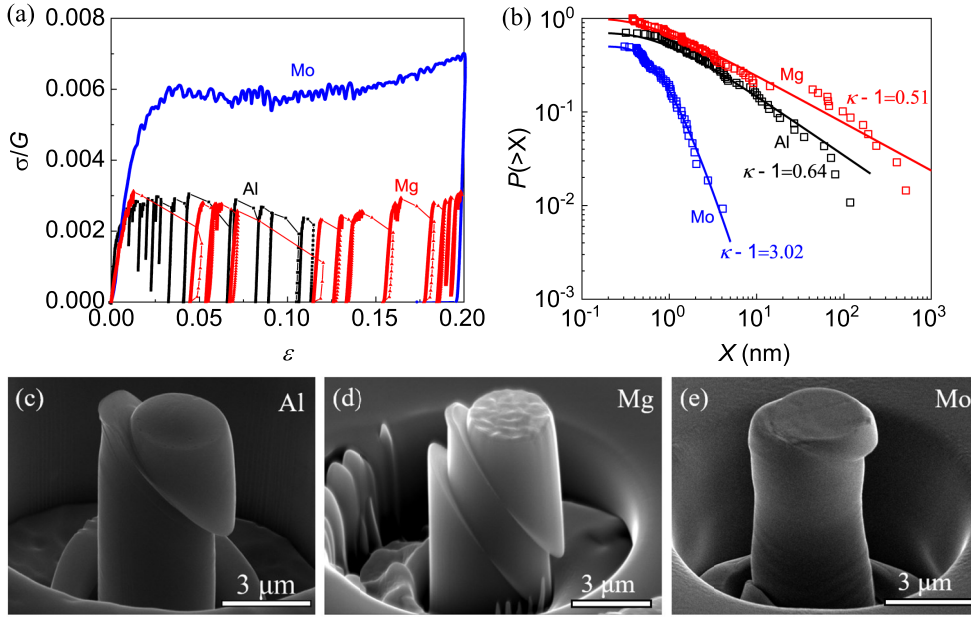


Figure 3. The effect of lattice structure on plastic fluctuations. (a) A comparison of stress–strain curves for 3500 nm pillars of three different materials, Mg (HCP), Al (FCC) and Mo (BCC). The stresses have been normalized by G , the shear modulus of each material. (b) Corresponding cumulative distributions of plastic displacements X over the entire loading. The solid lines represent the fit of the data with (2), and the corresponding lower cut-off values X_0 are 0.50 nm (Mg), 1.02 nm (Al) and 2.07 nm (Mo). (c)–(e) SEM images of (c) Al, (d) Mg and (e) Mo micropillars after compression. Single slip is observed for Al and Mg, while isotropic deformation is observed for Mo.

the temperature dependence of lattice friction and the limited ability of screw dislocations to cross-slip at low temperatures [25, 115]. In this case, we can define $l_d = 1/\sqrt{\rho_f}$, which means that we link the internal scale with the dislocation mean free path. However, the relation between l and l_d over a large range of conditions is not simple. On the one hand, increasing the lattice friction enlarges τ_{pin} , hence lowers l . On the other hand, the constant α_f in Taylor’s relation, $\tau_f = \alpha_f G b \sqrt{\rho_f}$, is smaller than 1.

In FCC materials, lattice friction plays a minor role, and the link between l_d and a dislocation mean free path is less direct (e.g. [116]). Indeed, dislocation patterning emerges naturally in these materials and the corresponding characteristic scale l_p (e.g. cell size) appears as a natural mean free path. The “similitude principle” then states [25, 32]

$$\frac{\tau_{\text{pin}}}{G} = k \frac{b}{l_p}, \quad (6)$$

which, combined with (4), relates l_p to our internal length scale

$$l_p = k \frac{Gb}{\tau_{\text{pin}}} = kl, \quad (7)$$

where k is a dimensionless constant; a comparison of experimental data for different materials suggests that $k \approx 7.5$ [25].

Similar reasoning can also help to rationalize the effect of crystal symmetry on plastic intermittency and the associated dislocation morphologies. We have already discussed above the systematic differences between FCC and BCC crystals. Figure 3 shows the results for HCP materials. We deal here with 3500 nm pillars of Mg. The observed mechanical response is extremely jerky, represented by a succession of plastic avalanches, which are power-law distributed in size with $\kappa \approx 1.5$. These observations for micropillars are entirely consistent with the recorded behavior of HCP bulk materials, where plastic jerkiness has been noticed long ago. It was seen directly on stress strain curves obtained for thin rods [1, 71], and was later quantified based on AE measurements for general samples [3, 33, 62, 82]. All these studies revealed a high degree of wildness $W_{AE} \approx 1$ independently of which HCP single crystals were studied (ice, Zn, Cd). The associated exponent for the distribution of AE energies was found to be very close to the mean field value 1.5.

These observations suggest an absence of the size-induced BD transition for HCP materials. Apparently, they remain in a critical state starting from the system size of a few μm and all the way to bulk scales. To rationalize these observations within our framework, we recall that the mentioned HCP materials are characterized by a very strong plastic anisotropy: gliding in such materials takes place preferentially along the basal planes whatever the system size. Another characteristic feature is a low Peierls stress and the associated lack of lattice friction. In other words, our parameter τ_l in such materials is anomalously small [25, 33]. Plastic anisotropy implies an absence of forest hardening, which means that τ_f is also negligible. Altogether this means that τ_{pin} is sufficiently small for l to be comparable to L . Then long-ranged elastic interactions fully control the collective dynamics and nothing prevents self organization of dislocations towards a critical state along the whole range of system sizes. The above arguments can explain the absence of a ductile/subcritical regime. The possibility of a super-critical regime in these materials is also very small because it requires an initially dislocation-free environment, which can be achieved only if the system size is decreased well below few μm .

The plastic anisotropy of Mg pillars is apparent in Figure 3(d) showing a single slip morphology. In fact, a strong correlation between plastic anisotropy and criticality should be kept in mind. As we have seen whatever the material and its crystal symmetry, either critical or supercritical regimes strongly correlate with slip anisotropy (see Figures 1(c, d), 2(c, d), 3(c, d)). Instead, ductile behavior can be associated with homogeneous deformation resulting from isotropization due to multislip (e.g. Figures 1(e) and 3(e)). In other words, there is a strong link between the dominance of short-range interactions, multislip and ductility (or subcriticality). In contradistinction, initial purity, dominant long-ranged interactions and extreme slip anisotropy, correlate with brittleness (or supercriticality). In these systems, however, supercriticality easily turns into a scale free behavior over the whole range of observable in the presence of a non-vanishing initial dislocation density.

In the next section we show how the above arguments transform in the context of plastic flows in alloys (see below) [64].

3. Alloys

The introduction of impurities has been used for millennia in classical metallurgy to harden bulk materials (e.g. [117]). Following this logic, the “smaller is stronger” size effect occurring in pure metals at μm and sub- μm scales, also appears beneficial. However, as we detailed above, such effect at small scale is accompanied by a detrimental “smaller is wilder” effect. The latter is culminating in brittleness at nanoscale (see above), which may compromise the forming processes and endanger the load-carrying capacity in various engineering/industrial processes taking place in such samples [37, 118]. A key challenge is therefore to develop new metallurgical

procedures to mitigate the associated plastic instabilities and reduce/suppress their detrimental effects, while preserving all the advantages related to high strength.

Studies revealed a much weaker size effect on strength in alloys compared with pure materials. This was interpreted as the fingerprint of a tailored internal length scale, which also suggested the possibility of the reduction of plastic intermittency [119–121]. The framework proposed in Section 2.4, and particularly our equations (4) and (5), can be used to rationalize these observations.

Indeed, the observations suggest an increase of the mean-field pinning strength τ_{pin} as the addition of solutes (τ_s) or precipitates (τ_p) should reduce the scale l . Since the latter controls the transition from a long-ranged to a short-range controlled dynamics, alloying expands the range of system sizes L over which plastic fluctuations remain mild.

Our own experiments on micropillars of Al alloys also confirmed the correctness of this interpretation [64]. Micropillars containing either clusters of Sc solutes (so-called Al–Sc cluster alloy), Al_3Sc precipitates (Al–Sc precipitate alloy), and θ' - Al_2Cu plate-like precipitates (Al–Cu–Sn alloy) were tested. They are characterized by an increasing pinning strength τ_{pin} that can be estimated from tensile tests at bulk scale. Figure 4(a) clearly shows that such alloying can strongly reduce wild, unwelcome plastic fluctuations, while preserving a strengthening effect. At the level of an individual alloy, the “smaller is wilder” effect is still present (Figure 4(b)). Therefore, even if it has been shown that alloying can weaken or even suppress the size effect on strength [119, 120], an effect on plastic fluctuations remains. However, in alloys this effect is definitively shifted towards smaller system sizes comparing to pure materials.

The distributions of displacement burst sizes X in the studied alloys were shown to be of mixed character, very well described by the generic expressions (1)–(2). The associated exponent κ and the characteristic size X_0 increase with increasing sample size L and pinning strength τ_{pin} (Figure 4(c)). We did not detect any signs of super-criticality over the analysed L -range, which is not surprising, given that the associated transition towards pure brittleness is not observed in our pure Al samples either, down to $L = 500$ nm.

In Section 2, we argued that the ratio of length scales $R = L/l$ is the key controlling factor of the wild-to-mild transition. We also concluded that there exists a universal (material-independent) relationship between wildness W and the corresponding exponent κ (3). Figure 5 shows the remarkable precision of these predictions.

When plotted as a function of the system size itself, the values of wildness parameter get shifted towards smaller L when we increase the pinning strength of extrinsic disorder (Figure 5(a)). However, a normalization of L by the internal scale $l = Gb/\tau_{\text{pin}}$ collapses the data for pure Al and for the different alloys of Al on the same curve. It shows that a wild-to-mild transition indeed takes place around $R \sim 1$ (Figure 5(b)). This prediction was also checked for the other materials tested, in particular, for Mo (BCC metal), which confirmed its generality. Figure 5(c), compiling W and κ values obtained for sample sizes ranging from sub- μm to bulk scales (in case of ice), various pure materials with different crystal symmetries, as well as different FCC (Al) alloys, illustrates the robustness of (3). The obtained agreement with observations indicates a sound basis of the underlying theoretical ideas. While the individual scaling exponents turn out to be nonuniversal [62, 67], the ensuing dependence of exponents on wildness appear to be universal. The theoretical ideas behind the proposed framework, which justify such a generalized notion of universality, will be discussed in Section 5.

Here, we also mention that the correlation between the anisotropy of the deformation morphology and the wildness, observed in pure materials, is also recovered in alloys (Figure 4(d)). In particular, the extrinsic factors which contribute to isotropy and promote multi-slip, also decreases the wildness [64]. These results suggest that wild plastic intermittency, implying unwelcome large fluctuations, can be systematically subdued from a tailored set of homogeniz-

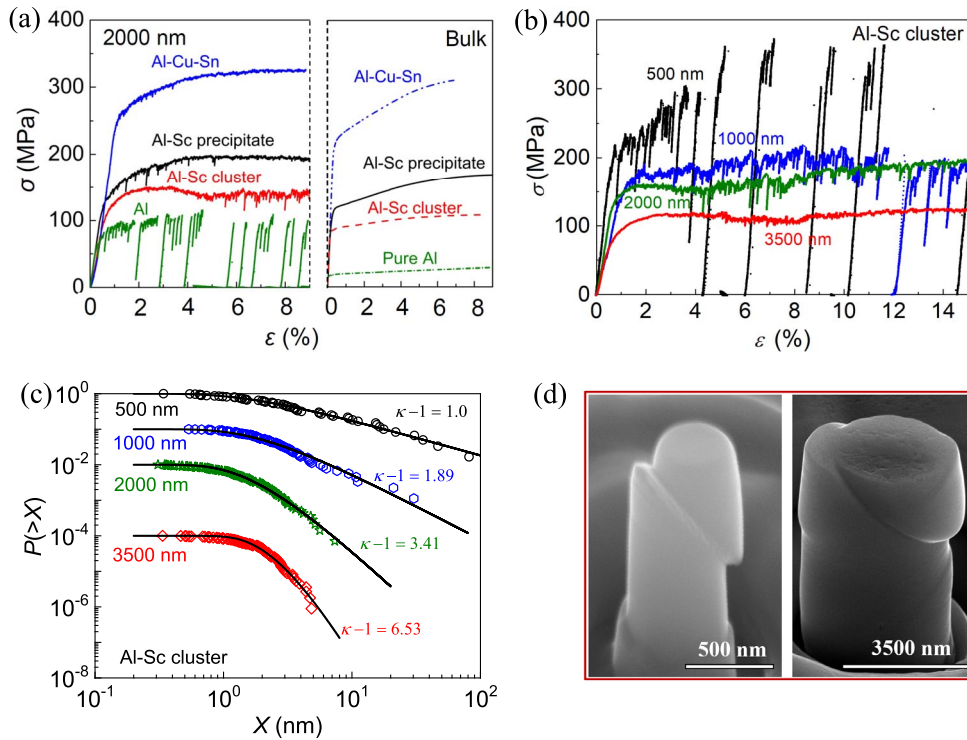


Figure 4. Taming plastic fluctuations from alloying: the case of Al-Sc alloys. (a) Stress-strain curves for pure Al and Al alloys. (b) Stress-strain curves for Al-Sc cluster pillars of different diameters. (c) Corresponding cumulative distributions of plastic displacements X over the entire loading. The solid lines represent the fit of the data with (2), and the corresponding lower cut-off values X_0 are 1.91 nm (500 nm pillar), 3.16 nm (1 μ m pillar), 4.11 nm (2 μ m pillar), and 11.2 (3.5 μ m pillar). (d) SEM images of a 500 nm pillar (left) and a 3500 nm pillar (right). Single slip is observed for the small pillar, and multislip for the large one. Adapted with permission from [64].

ing defects, at least in FCC materials. The possibility of extending these wildness suppression techniques to other crystalline structures, and, in particular to HCP materials displaying plastic jerkiness even at macroscales [1, 33, 71], remains to be explored.

In the studied FCC alloys, τ_{pin} , and therefore the internal scale l , are largely controlled by the extrinsic disorder terms τ_s and τ_p . These parameters depend on both the pinning strength of individual obstacles and their average spacing λ . In the studied samples the spacing λ was always smaller than l , sometimes (Al-Sc cluster alloy) by more than an order of magnitude. Therefore, λ is not an appropriate normalization scale to reveal the underlying wild-to-mild universality. In all cases, λ was also much smaller than L , justifying our approximate formula for τ_{pin} . One can wonder what would happen when $\lambda \sim L$, i.e. when dislocations can potentially cross over the system without meeting an obstacle. Will this eliminate the beneficial effect of alloying and open the way towards supercriticality and brittleness?

While these questions remain essentially open, we can refer to our recent work on Al-Cu alloys with much larger θ' -Al₂Cu plate-like precipitates, i.e. of diameter d_p commensurate with the size of the micropillars [68]. In that case, our simplified picture breaks down. In particular, comparing to alloys with much smaller obstacle sizes but a similar τ_{pin} (deduced from tensile test at bulk

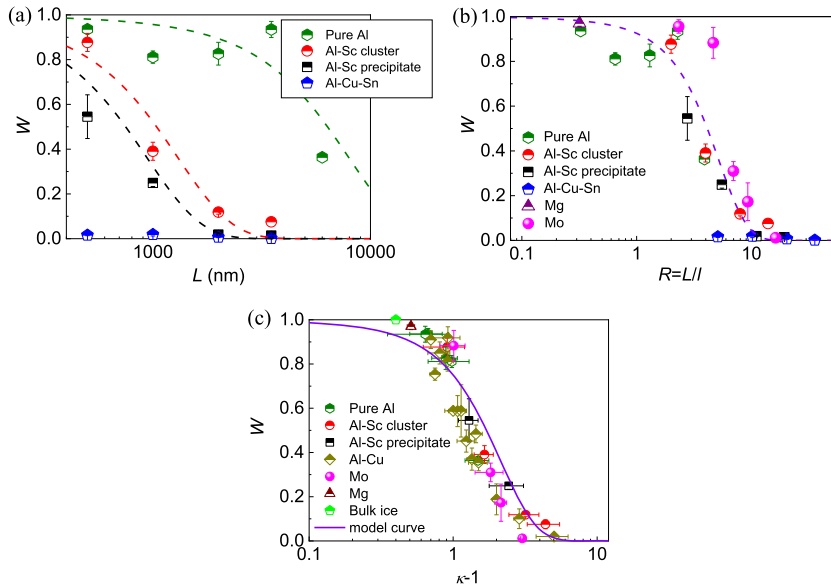


Figure 5. The universal character of the wild-to-mild transition. (a) Wildness W as a function of pillar diameter L for pure Al and various Al-alloys with increasing pinning strength. (b) Wildness W as a function of the dimensionless ratio $R = L/l$ for different pure materials and alloys, where l was computed from (4) using τ_{pin} values estimated from tensile tests at bulk scales, except for Mg for which the lattice resistance of basal slip was used, i.e. $\tau_{\text{pin}} = \tau_l = 0.5$ MPa. (c) The universal relationship between wildness W and the exponent κ .

scales), the ensuing plastic flows are much wilder. A sharp decrease of wildness was observed over an intermediate range of system size, when $d_p \approx L$ and the precipitates cut the entire micropillar. Despite the implied modification of the pinning picture, the statistic of plastic fluctuations in these alloys remained consistent with the proposed W versus κ relationship (3), which should be viewed as another manifestation of its universal character.

4. Wildness versus strength

In the discussion above, we assumed that in pure materials with low lattice friction, the parameter τ_{pin} is mainly controlled by forest dislocations. More specifically, we argued that the term $\tau_f \sim Gb\sqrt{\rho_f}$ must be tightly linked to Taylor's forest hardening. This idea is supported by the extreme wildness of pure divalent HCP metals (Mg, Zn, Cd) and ice, even at macroscopic scales [1, 3, 33, 71, 82]. It is illustrated in Figure 5(c), where we see that $\kappa \approx 1.5$ and $W \approx 1$. We recall that in such materials, plastic deformation is strongly anisotropic, with preferential glide along the basal plane and a correspondingly very small Peierls stress τ_l [25, 33, 122]. The strong plastic anisotropy implies an absence of forest hardening, i.e. a possibility to completely neglect τ_f . In fact, both effects conspire to ensure a large value of l and therefore a wild behavior over an extended range of system sizes.

Note, however, that other HCP metals, such as Ti and Zr, preferentially glide along prismatic planes. They also exhibit a considerable temperature-dependent lattice friction for screw dislocations below an athermal transition temperature [25]. The impact of these and other specific features of some HCP materials on the jerkiness of plastic flow remains to be fully explored. Note

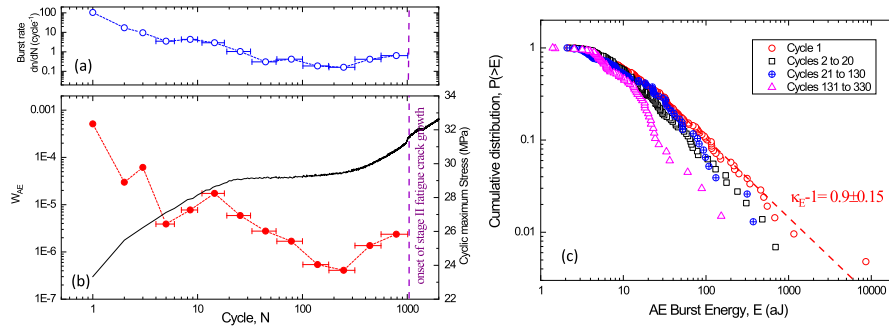


Figure 6. Cyclic strain-controlled tension-compression test ($\epsilon_{\min}/\epsilon_{\max} = -1$; $\Delta\epsilon = 0.95\%$) on an annealed Al sample. The cyclic stress response (csr-curve) is shown as a black line on panel (b), showing an initial hardening stage over the first ~ 30 cycles. The AE burst rate (number of discrete bursts per cycle) is shown on panel (a), while the wildness proxy W_{AE} is shown on panel (b) with red closed circles. (c) Cumulative probability distributions of AE burst energies at different stages of cyclic deformation and hardening. Adapted with permission from [66]. Copyrighted by American Physical Society.

that prismatic glide in Ti, unlike Zr, proceeds through a locking-unlocking mechanism related to the relative stability of the dislocation core, therefore appears intrinsically jerky [123]. However, the link between this intrinsic jerkiness and the one mainly discussed here, i.e. resulting from a collective dynamics, is still an open question.

On the other hand, FCC metals are the paradigmatic forest-hardening materials. Here one can expect a strong link between dislocation patterning, hardening rate, and plastic fluctuations and for pure Al [66] and Cu [69] the implied interrelationships were recently analyzed at bulk scales. Cyclic loading was imposed and plastic bursts were tracked with wildness estimated from AE. As illustrated in Figure 6, in Al, both the number of detected AE bursts per cycle and the wildness measure W_{AE} are correlated with hardening. More specifically, in these cyclic strain-controlled tension-compression tests, the initial cyclic hardening stage, lasting about 30 cycles, is accompanied by a strong decrease of the burst activity (Figure 6(a)) and the drop of W_{AE} (Figure 6(b)). Instead, the exponent of the power law tail of AE energy distribution progressively increases (Figure 6(c)). This is consistent with our theoretical predictions, as strain hardening and the associated increase of τ_f suggest the decrease of l which makes plastic flow milder. The results shown on Figure 6 were obtained for annealed Al samples. Measurements performed on non-annealed samples with a larger initial forest dislocation density revealed a similar trend, however with a much smaller initial (1st cycle) wildness W_{AE} , still in agreement with our picture [66].

Cyclic stress-controlled tests performed on pure Cu, combined with electron back-scattered diffraction (EBSD) and rotational-electron channeling contrast imaging (R-ECCI) observations, shed additional light on the relationship between dislocation patterning and plastic fluctuations [69]. These tests involved several cyclic steps with increasing stress amplitudes, which were performed on a same sample. During a single step with fixed stress amplitude, the evolution of plastic fluctuations was fully consistent with what we described above for Al, including strain hardening and progressive formation of a dislocation substructure accompanied with a decrease of wildness. A correlation was observed between the dislocation mean-free path l_p , estimated from R-ECCI at the end of each cyclic step, and the value deduced from the continuous AE. The latter was interpreted as resulting from the cumulative effect of numerous uncorrelated dislocation motions over sweeping areas $A \sim l_p^2$.

However, it was noticed that upon increasing the stress amplitude, the previously built dislocation patterns are destroyed while new ones are rebuilt. Such major restructuring takes place over just few loading cycles. The associated destabilization occurred, at least partly, through dislocation avalanches that propagated much further than the scale l_p generated at the previous stage. In addition, in all the cyclic experiments mentioned above, rare AE bursts were recorded even during the stage of hardening saturation presumably associated with very stable dislocation substructures. This suggests an ultimately metastable character of these patterns, making them susceptible to episodic large rearrangements spanning over scales much larger than l_p [62, 66].

Based on the results obtained in a continuum model of plasticity [65] and the associated simulations in the framework of discrete dislocation dynamics (DDD) [36], it was proposed that strain hardening introduces an *upper* cut-off s_* to the distribution of dislocation avalanche sizes. It would then write $P(s) \sim s^{-\kappa} f(s/s_*)$, with $f(x)$ a cut-off function rapidly decaying for $x > 1$. The prediction was that s_* is inversely proportional to the system size L (finite-size effect) and to the hardening coefficient. This conclusion can justify the decrease of the energy released in plastic avalanches as the material strain-hardens. However, it does not explain the concurrent proliferation of mild fluctuations associated with a degeneration of the *lower* size tail of the power law avalanche distribution. In fact, the effect of hardening on this lower cut-off avalanche scale (X_0 in (1)) remains an open question.

In the considerations presented above, strain hardening in FCC bulk materials was analyzed in the conditions where Taylor's forest hardening was the most relevant mechanism. However, upon decreasing the system size below few μm , a breakdown of this size-independent mechanism can be envisaged. It can be expected to be replaced by source-dominated mechanisms responsible for the "smaller is stronger" size effect [124]. In this case, the usual weak bulk dislocation sources are almost absent and much higher stresses are required, in average, to activate the much stronger, surface controlled sources [97]. In such regimes, where isolated breakthrough events dominate, an increasing scatter of strength measurements can be also expected.

This transition from bulk to surface sources can be linked to the transition from short-range controlled (allowing forest hardening) to long-range controlled (through distant surfaces) dynamics. Moreover, both transitions can be now interpreted in terms of our dimensionless ratio $R = L/l$ [125], which was shown to regulate the apparently unrelated mild-to-wild transition.

In this perspective, one can anticipate a relation between the disappearance of forest hardening, the emergence of a size effect on strength, and the new "smaller is wilder" size effect. The analysis of compression tests on Al and Al-alloys micropillars allowed us to actually establish such a relation [64].

More specifically, we compared the strain hardening rate (SHR) of our pillars, Θ_{pillar} , with those for the same material at bulk scales, Θ_{bulk} . We observed a ratio $\Theta_{\text{pillar}}/\Theta_{\text{bulk}} \simeq 1$, i.e. a persistence of Taylor's hardening, down to $R \simeq 5$, but much larger and more scattered values at smaller system sizes (Figure 7). Characteristically, the associated transition took place concomitantly with the mild-to-wild transition (Figure 5). The observed correspondence extends also to alloys where extrinsic disorder shifts the transition from forest to source exhaustion hardening towards smaller system sizes. Since the effect of disorder is the same on the mild-to-wild transition, one can argue for the close relation between the underlying transition. The disappearance (or at least the weakening) of size effect on yield stress in alloys in the μm system size range [119, 120] is also fully consistent with this scenario.

Finally, we mention that with decreasing the system size further, another relation between the fluctuations and the size effects on strength apparently emerges. Thus, in Au (FCC) nanoparticles with $L \simeq 400$ nm, a saturation of the size effect on plastic yield was observed together with a brittle-like behavior (supercritical in our terms; see Section 2.2). These observations were interpreted in terms of a transition from source-exhaustion/truncation hardening mechanism

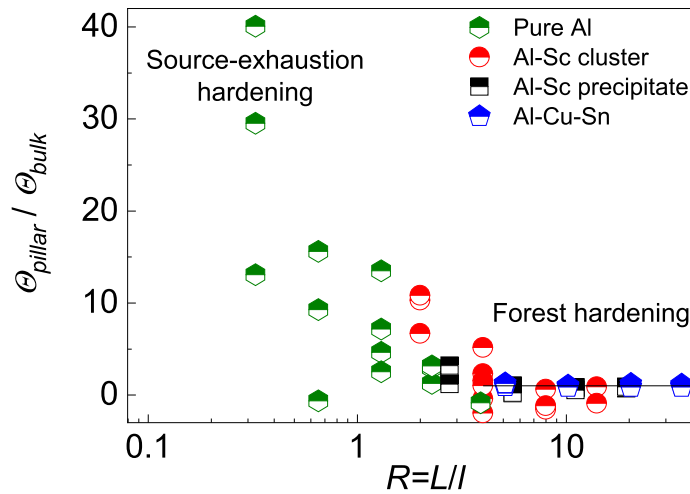


Figure 7. The hardening transition in FCC (Al and Al alloys) micropillars. The normalized strain-hardening rate $\Theta_{\text{pillar}}/\Theta_{\text{bulk}}$ is shown as a function of the dimensionless ratio R . A transition from forest hardening to source-exhaustion hardening is observed around $R \simeq 5$, whatever the material, in excellent agreement with the mild-to wild transition in Figure 5(b). Adapted with permission from [64].

of plastic flow to a homogeneous dislocation nucleation mechanism [126]. Not surprisingly, in such regimes the yield strength was found to approach the theoretical strength of the material.

5. Modelling

The discussion above highlighted a rich landscape of plastic behaviors in crystalline materials, with the mechanical responses and the associated fluctuations depending on crystal symmetry, system size, and disorder (either quenched: solutes, precipitates, ..., or emergent: forest dislocations, dislocation patterns, ...). To rationalize these observations we consider below two types of modelling approaches: mesoscopic and mean field.

5.1. Mesoscopic model

We have shown above that the dimensionless ratio $R = L/l$ appears as the key controlling parameter, encompassing the external size effect (“smaller is wilder”) as well as the disorder through the internal scale $l \sim 1/\tau_{\text{pin}}$ [67]. Below, we show how the effects of system size and disorder can be analyzed in a single setting using a minimal model of crystal plasticity. The main idea behind this model is the reduction of the plastic flow problem to a computationally effective integer-valued *discrete automaton*. Despite the simplicity of the ensuing dynamical system, one can account in this way for both short-range and long-range elastic interactions, including dislocation nucleation and immobilization. It also allows one to accumulate sufficient statistics, since one can deal in this way with millions of mesoscopic elements and tens of thousands of dislocations.

The 2D version of this model was first introduced in [70, 127], and here we simply recall its main characteristics following [67]. The model assumes that the displacement field is scalar and that the flow is of single-slip nature. Hence, forest dislocations cannot be considered directly.

However, we recall that the plastic flow of sufficiently small micro-pillars is mainly single-slip independently of the underlying crystal symmetry. Even in the case of multi-slip orientation, due to a limited number of available dislocation sources within the confined volume, the first activated slip plane dominates and prevents other slip planes from getting involved. In this situation, the usual frustration leading to hardening can be avoided considering the absence of dislocation cross-slip and easy annihilation at a free surface. While any adequate crystal plasticity model would effectively reduce to our constrained single-slip theory in a sufficiently small system, it should, of course, allow for multi-slip flow to take over at larger sample sizes. In fact, a fully tensorial 2D model has been recently proposed, which allows the modelling of different crystal symmetries and multislip configurations [128], however at a much higher computational cost.

In the framework of the scalar model we essentially imply that the sample is oriented for a single slip along the only available slip direction. The crystal is modeled as an $N \times N$ square lattice with the mesoscopic spacing normalized to unity. The deformation of the crystal is given by the displacements of the vertices of the mesoscopic elements, $\vec{u}_{i,j} = (u_{i,j}^x, u_{i,j}^y)$, where $i, j = 1, 2, \dots, N$.

In view of the single slip assumption we can set $u_{i,j}^y \equiv 0$. We can then introduce the notation $u_{i,j} \equiv u_{i,j}^x$. In the presence of a kinematic constraint the strain tensor can be reduced to two fields: a longitudinal strain, $\zeta_{i,j} = u_{i+1,j} - u_{i,j}$, which is a linear, non-order parameter variable, and a shear strain $\xi_{i,j} = u_{i,j+1} - u_{i,j}$, which is a nonlinear, order parameter type variable, given that plastic slip originates from multi-well nature of lattice potential.

We write the dimensionless energy of the system in the form [70] $\Phi = \sum_{i,j} f(\zeta_{i,j}, \xi_{i,j})$, where $f(\zeta, \xi) = (K/2)\zeta^2 + f_0(\xi)$ is the energy of a single (meso-scope) element. To account for the lattice periodicity we assume that $f_0(\xi) = f_0(\xi + n)$, where $n \in \mathbb{Z}$ is an integer-valued slip. Moreover, for analytical transparency we assume that the *periodic* energy density f_0 is piece-wise quadratic $f_0(\xi_{i,j}) = (1/2)(\xi_{i,j} - d_{i,j}(\xi))^2$. Here the plastic slip d is represented by an integer nearest to ξ so that $d_{i,j}(\xi) = \lceil \xi_{i,j} \rceil$. The obtained model depends on a single dimensionless parameter K which mimics the ratios of elastic constants $(C_{11} - C_{12})/(4C_{44})$ or C_{11}/C_{66} . It describes the coupling between mesoscopic elements that carry different values of ξ . In the limits $K \rightarrow 0, \infty$ we obtain solvable 1D models with mean field type interaction [127, 129]. At $K \neq 0$ the model reproduces Eshelby-type propagator and therefore captures crucial effects of long range interactions induced by elastic compatibility, see more about this below. In our numerical experiments we assumed that $K = 2$ which represents a typical value for metallic crystals.

The model can be reduced to a discrete automaton because the elastic problem $\partial\Phi/\partial u_{i,j} = 0$ can be solved analytically if the integer-valued field d is known [70]. The associated equilibrium equations in the bulk, written in terms of the displacement field $u_{i,j}$, read

$$K(u_{i+1,j} + u_{i-1,j} - 2u_{i,j}) + (u_{i,j+1} + u_{i,j-1} - 2u_{i,j}) - (d_{i,j} - d_{i,j-1}) = 0. \quad (8)$$

The whole system can be written in matrix form $\mathbf{M}u = b$, where \mathbf{M} is a pentadiagonal matrix and b is a vector of size $N \times N$ incorporating the boundary conditions and the field d . The problem then reduces to a simple matrix inversion.

We assume periodic boundary conditions in the horizontal direction $u_{1,j} = u_{N+1,j}$. A hard device type loading is applied through the boundary condition in the vertical direction $u_{i,N+1} = u_{i,1} + \gamma$, where γ is the control parameter. Periodicity is assumed to allow for the fully explicit inversion of the matrix \mathbf{M} . Indeed, we can then use the spectral approach based on the Fourier transform $\hat{x}(\mathbf{q}) = N^{-2} \sum_{a,b} x_{a,b} e^{-i\mathbf{q}\mathbf{r}}$ with $\mathbf{r} = (a, b)$ and $\mathbf{q} = (2\pi k/N, 2\pi l/N)$. In Fourier space the solution of our linear problem is straightforward and we can obtain an explicit representation for the equilibrium shear strain

$$\hat{\xi}(\mathbf{q}) = \gamma \delta(\mathbf{q}) + \hat{L}(\mathbf{q}) \hat{d}(\mathbf{q}), \quad (9)$$

where we recall that $\gamma = \langle \xi \rangle$ is the measure of the imposed affine deformation. Here the sign-indefinite Eshelby-type kernel with r^{-2} far field asymptotics takes the form

$$\hat{L}(\mathbf{q}) = \frac{\sin^2(q_y/2)}{K \sin^2(q_x/2) + \sin^2(q_y/2)}. \quad (10)$$

Its dipolar structure reflects the *scalar* nature of our model; the more conventional quadrupole structure of the stress propagator is a feature of isotropic elasticity, while here we deal with the extremely anisotropic limit [130, 131].

Since we now know how to update the elastic fields, we can formulate the quasi-static athermal dynamics in the form of a discrete *automaton* for the integer-valued field d . We start with the unloaded ($\gamma = 0$) and dislocation-free state ($d_{i,j} \equiv 0$). We then advance the loading parameter γ and compute (predict) the elastic field $u_{i,j}$ while keeping the field $d_{i,j}$ fixed. The knowledge of the shear strain field $\xi_{i,j}$ allows us to update (correct) the plastic strain field using the relation $d = \xi$; the update takes place when the boundary of the energy well is reached by at least one of the mesoscopic elements. Then an avalanche occurs while we use synchronous dynamics for the updates of $d_{i,j}$. We repeat the prediction-correction steps at a given γ till the corrections stop changing the field $d_{i,j}$ and the system stabilizes in a new equilibrium state. As the stress in this state is globally below the threshold and we can start a new search for the increment of $\delta\gamma$ that destabilizes at least one unit. As soon as such an element with $d_{i,j} \neq \xi$ is obtained we apply our relaxation protocol again, initiating another avalanche. When avalanche finishes, the variation of γ resumes.

In (10), two types of quenched disorder can be introduced [67]. The *nonlocal* disorder field h mimics the effect of elastically incompatible impurities such as solutes. The *local* disorder g can be viewed as resulting from lattice-compatible obstacles with only a local effect on plastic slip such as e.g. locked dislocation multipoles whose long-ranged fields are screened. The energy density accounting for both types of disorder takes the more symmetric form [70, 127]:

$$f(\xi_{i,j}, \zeta_{i,j}) = \frac{K}{2} \zeta_{i,j}^2 + \frac{1}{2} (\xi_{i,j} - d_{i,j}(\xi))^2 - h_{i,j} \zeta_{i,j} - g_{i,j} \xi_{i,j}. \quad (11)$$

Both disorder fields, h and g , can be assumed as drawn independently in each lattice cell from Gaussian distributions $p_s(r) = (2\pi\delta_s^2)^{-1/2} \exp(-r^2/(2\delta_s^2))$, where $s = (g, h)$. The specificity of the disorder $g_{i,j}$, representing essentially a residual plastic strain, is that it can be simply combined in the energy density with the actual plastic strain $d_{i,j}$. For instance, to account for g in the Fourier representation of the elastic solution, it is sufficient to replace the field $\hat{d}(\mathbf{q})$ by the sum $\hat{g}(\mathbf{q}) + \hat{d}(\mathbf{q})$. We can then write

$$\hat{\xi}(\mathbf{q}) = \gamma \delta(\mathbf{q}) + \hat{L}(\mathbf{q})[\hat{d}(\mathbf{q}) + \hat{g}(\mathbf{q})] + \hat{L}_h(\mathbf{q}) \hat{h}(\mathbf{q}), \quad (12)$$

where

$$\hat{L}_h(\mathbf{q}) = \frac{\sin(q_x/2) \sin(q_y/2) \left(\cos\left(\frac{q_x - q_y}{2}\right) - i \sin\left(\frac{q_x - q_y}{2}\right) \right)}{K \sin^2(q_x/2) + \sin^2(q_y/2)} \quad (13)$$

is a distorted Eshelby propagator (10) maintaining, however, its sign-indefiniteness and the decay rate $1/r^2$.

Below we first show some of our simulation results for the case of nonlocal disorder h . In all numerical experiments we considered initially dislocation-free systems ($d \equiv 0$), and the statistical results were averaged over at least 100 realizations of the disorder. Figure 8 shows the average mechanical response of our system under simple shear as well as the evolution of the yield strain γ_y as a function of the disorder variance $\delta_h = \delta$ under the assumption that $\delta_g = 0$. For weak disorder, $\delta \leq 0.3$ (regime A on Figure 8), mimicking initially dislocation free, almost pure and small crystals, yielding is brittle-like, with an abrupt stress drop and a strong strain localization along a shear band which concentrates the dislocations [67] (panel (A) on Figure 8). This regime

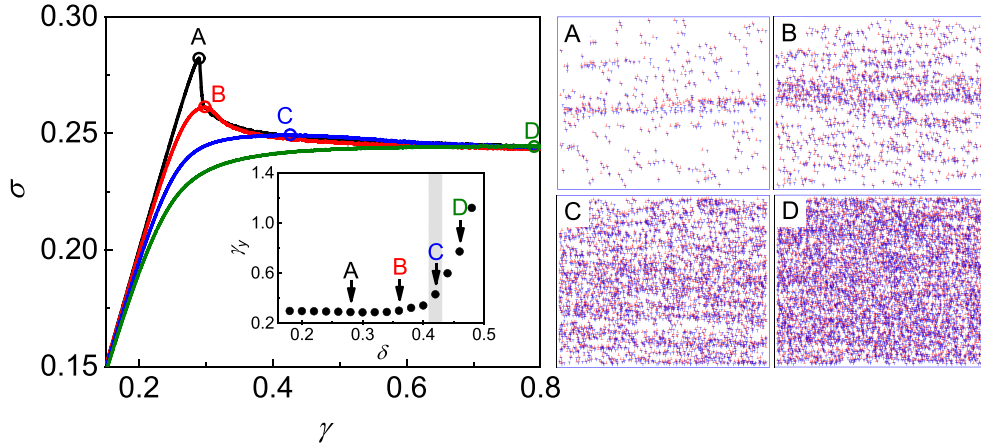


Figure 8. The effect of disorder on average stress–strain curves in simple shear simulations ($N = 1024$). The inset shows the yield strain γ_y , with the grey strip marking the extended BD transition. Panels A–D show zooms on the corresponding post-yield dislocation configurations. Adapted with permission from [67]. Copyrighted by American Physical Society.

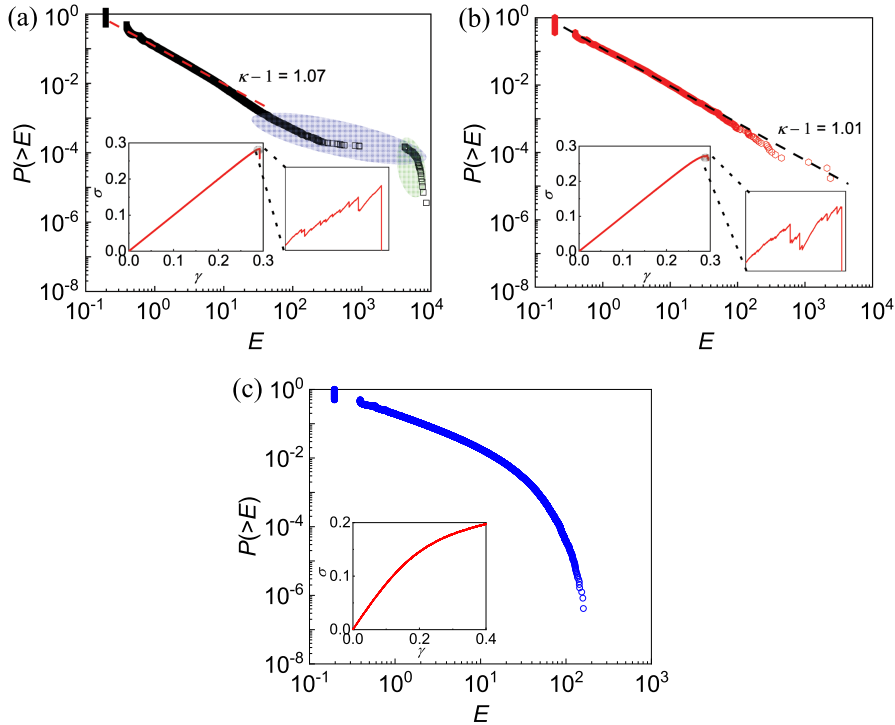


Figure 9. Cumulative probability distributions of preyield avalanche energies at $\delta = 0.28$ (a), $\delta = 0.32$ (b) and $\delta = 0.7$ (c). Averaging was performed over 100 realizations of the disorder. Insets show stress–strain curves for a particular realization of the disorder. Adapted with permission from [67]. Copyrighted by American Physical Society.

is reminiscent of the brittle behavior of nanoparticles prepared from solid-state dewetting, i.e. initially dislocation free [93, 103, 126], or of our smallest Mo pillars (Figure 1).

Upon increasing the disorder, the first-order transition eventually terminates at a critical point located around $\delta \simeq 0.42$ (regime C), in a way similar to what has been identified in amorphous plasticity [132]. In this regime, the plastic slip field $d_{i,j}$ is scale-invariant, characterized by a turbulent-like multifractal pattern [67], qualitatively consistent with the spatial fractal pattern of plastic bursts observed from AE in a bulk ice crystal [81]. At even larger disorder, $\delta \geq 0.5$ (regime D), yielding is gradual and the mechanical response is ductile, with both dislocations (Figure 8 (panel D)) and slip uniformly distributed within the whole crystal [67].

The correspondence with experiments can be also established in terms of statistics of plastic fluctuations. In our automaton model, the energy E released during an avalanche scales with the cumulative distance covered by all the moving dislocations involved [67, 127], i.e. with the displacement X as defined above. Hence, computed energy distributions $P(E)$ and experimental distributions $P(X)$ are directly comparable. At small disorder, the model captures the coexistence of dragon-king outliers with power-law distributed smaller avalanches characterizing a supercritical regime (Figure 9(a)), as observed in our 500 nm Mo pillars (Figure 1(a)). Upon increasing δ , a critical regime emerges (Figure 9(b)), with a power law distribution of avalanches energies and an exponent κ consistent with that observed for Mo pillars of intermediate sizes (Figure 1(b)). At even larger disorder, scaling disappears and subcritical statistics are obtained (Figure 9(c)). This general agreement with observations argues for the robustness of the different regimes identified above, as well as the transitions between them, upon increasing the system size and/or the disorder strength.

In fact, we argue that by varying the strength of quenched disorder one can differentiate between sub-micron crystal sizes. Indeed, instead of L we should use a dimensionless parameter $R = L/l$ introduced earlier. If we assume that $l \sim Gb/\sigma_{th}$ identifies the threshold σ_{th} with the pinning (immobilization) stress, we can recall that the distinctly brittle regime would correspond to $R \ll 1$, the strongly ductile regime, to $R \gg 1$, while dislocation interaction with obstacles would become relevant at $R \sim 1$. The threshold σ_{th} naturally depends on the presence of the pinning obstacles and, in general [64], increases with the variance of quenched disorder imitating such obstacles. More specifically, the decrease of σ_{th} can be achieved by making the disorder more narrow which can be viewed as the way to eliminate particularly strong obstacles. In this way, instead of increasing L we can decrease l , which should be as effective in moving from the brittle regime, where $R \ll 1$, to the ductile regime, where $R \gg 1$. In other words, instead of exploring directly the dominance of surface effects one can exploit the indirect effect that in smaller systems there are fewer strong obstacles that can serve, for instance, as dislocation nucleation sites because the existing ones are compromised or even disabled by their closeness to the surfaces.

It has to be mentioned, however, that our association of the variance of disorder with crystal size is exclusively targeting systems without bulk criticality, as in the case of Mo crystals. One can, in principle, manufacture small crystals with strong (dense) quenched disorder [64] or grow almost pure large crystals with very weak (sparse) quenched disorder [33]. In general, both quenched disorder and the crystal size would affect brittleness, even though to grow almost defect free crystals (without solutes, precipitates and dislocations), is almost impossible except in case of extremely small sizes (nano-particles).

In Figure 9 we showed stress-*integrated* distributions of plastic fluctuations collected over the entire pre-yield loading. However, a detailed interpretation of the nature of these fluctuations generally requires an analysis of stress-*resolved* distributions. As an example, a stress-tuned criticality (e.g. depinning) would be characterized by $P(E) \sim E^{-\tau} f(E/E_c)$, where $f(x)$ rapidly vanishes for $x > 1$ and E_c is an *upper* cut-off that diverges at a critical stress σ_c , such that $P(E) \sim E^{-\tau}$ only at the critical point $\sigma = \sigma_c$. Note that in this case the stress-integrated exponent κ differs from the stress-tuned exponent τ . It has been argued that the plasticity of micropillars

could belong to such stress-tuned criticality [5, 78]. This interpretation is however disputed [50], while the analysis of stress-resolved distributions might be difficult owing to a lack of statistics. AE data collected on bulk samples furnish larger catalogs that instead argue against tuned criticality [2, 3, 82], at least in HCP materials.

Taking advantage of the low numerical cost of our simulations, we performed a detailed analysis of stress-resolved distributions for the released energies E in our scalar model on the basis of extended statistics. Figure 10 shows the evolution of immediately pre- and post-yield exponents, along with some examples of corresponding distributions. From these results as well as additional analyses detailed elsewhere [67], different types of critical behavior can be identified as a function of disorder strength δ mimicking also the system size (see above).

At very small disorder ($\delta \simeq 0.2$), supercriticality and strong brittleness is characterized by small and similar pre- and post-yield exponents, $\tau \simeq 1$. This allows one to draw an analogy with marginal stability of spin glasses [133]. In this case, homogeneously nucleated dislocations self-organize under the influence of long-ranged elastic forces and the system undergoes a transition from a stable (elastic) to a marginally stable (glassy) state.

Over an intermediate disorder range ($0.25 < \delta < 0.35$), a gap opening is observed between the pre- and post-yield exponents, and a characteristic peak is still observed in the post-yield distribution (Figure 10(c)). A scaling collapse analysis reveals a *tuned* spinodal criticality in this regime, with an upper cut-off E_c diverging as approaching the yield stress as $E_c \sim (\sigma_y - \sigma)^{-1/\nu}$, however with an exponent $1/\nu \simeq 1.6$ different from the mean-field depinning prediction $1/\nu = 2$ [79, 134] (Figure 10(d)). This suggest that tuned-criticality could be indeed relevant for the plasticity at small system sizes [5]. We recall however that our modelled systems are initially dislocation-free, which is hardly the case in micropillar experiments, at least for FCC light materials (see Section 2.3). When performing cyclic loading at these levels of disorder with our model, the post-yield stress drop as well as the associated super-critical avalanches disappear from the first loading reversal, i.e. the distributions becomes critical [67]. This strongly suggests that spinodal tuned-criticality is suppressed when reloading a dislocation-rich system. In other words, a potentially brittle nanocrystal could be “trained” to become more ductile from gentle cyclic loading, with potential applications in nano-engineering.

Note that the spinodal critical regime is only observed over a limited range of disorder. At larger disorder ($\delta \sim 0.42\text{--}0.46$), the BD transition takes place, with the post-yield stress drop as well the characteristic peak in the distribution disappearing, and pre- and post-yield collapsing (Figure 10(a)). This second-order BD criticality is associated with a cut-off following a different asymptotics, $E_c \sim \exp(\sigma/\sigma_0)$, where σ_0 is a constant (Figure 10(e)), meaning that criticality is not stress-tuned in this case [50]. Finally, upon increasing further the level of disorder beyond $\delta \simeq 0.5$, “hardening” takes place almost from the onset of loading, plastic activity becomes homogeneous and uncorrelated, and scaling is getting lost.

To summarize, our numerical studies, consistently with the experimental observations reported above, reveal an extremely rich repertoire of plastic behaviors. An evolution from a typically brittle behavior (though without cracks) to a mostly ductile response can be conceptualized as a complex three-stage crossover: a spin-glass-type marginality encountered for very small, almost disorder-free crystals, transitions to a spinodal stress-tuned criticality at an intermediate level of disorder, then followed by a second-order BD transition at larger disorder (and/or size), to finally a lack of scaling and a fully ductile behavior at very large disorder/scale. This scenario shows some similarity with what has been recently proposed for amorphous plasticity [132, 135], although crystalline plasticity appears even more intricate. In this framework, scaling laws and exponents are non-universal.

We now briefly illustrate the interplay between our two types of disorder, “local” and “nonlocal”. To avoid the dependence on the initial preparation we have now choose the setting of cyclic

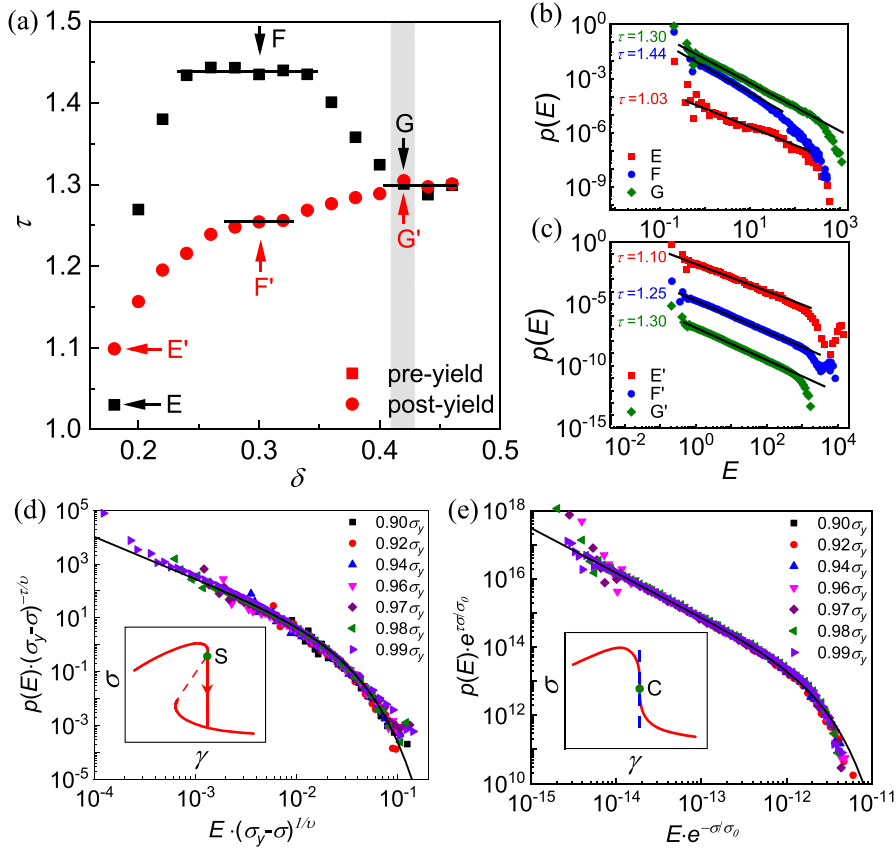


Figure 10. (a) Disorder dependence of the stress-resolved scaling exponent τ for immediately pre- and post-yield situations. The gray strip marks schematically the extended BD transition. (b, c) Corresponding avalanche energy distributions. The scaling collapse of the preyield distributions are shown (d) for $\delta = 0.30$ (tuned spinodal criticality) and (e) $\delta = 0.46$ (BD criticality). Adapted with permission from [67]. Copyrighted by American Physical Society.

loading. Our numerical experiments, summarized in Figure 11(a), show that when a weak “local” disorder $\delta_g = 0.3$ is combined with a weak “nonlocal” disorder $\delta_h = 0.3$, the overall mechanical response is ductile. The initial softening behavior, observed in crystals with $\delta_g = 0$, is replaced by the more conventional hardening behavior. At large strains the stress response shows a robust yielding plateau independently of the configuration of disorder. The overall response is reminiscent of the classical strain-hardening behavior exhibited by *bulk* FCC and BCC materials [136].

From Figure 11(b) we see that even a weak “local” disorder is sufficient to suppress supercriticality and to completely eliminate system-size events. This observation agrees with the idea that such disorder generates local inhomogeneities which inhibit global response. However, the increase of the cut-off size in the second cycle suggests that a correlated behavior, reminiscent of disorder-induced self-organization towards classical criticality in RFIM (random field ising model) [137, 138], can still take place.

In Figure 12 we show how the different configurations of “local” and “nonlocal” disorder strengths affect the cycle-averaged (integrated) scaling exponents τ_{in} . When the “local” disorder

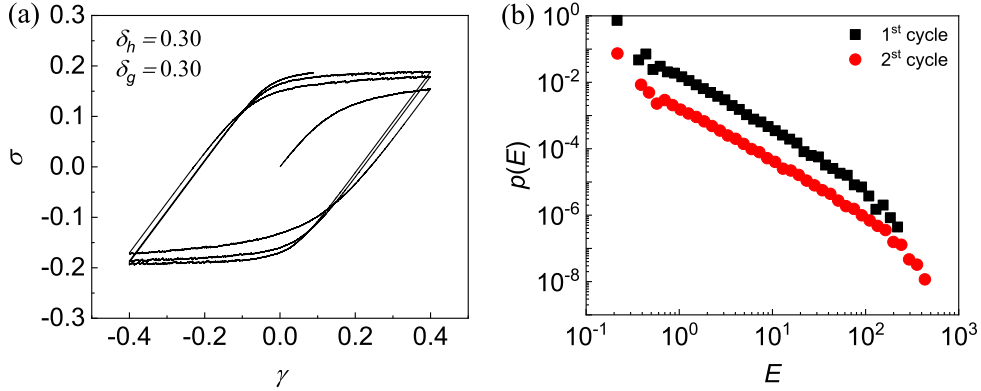


Figure 11. (a) Strain–stress curves for the crystals subjected to six loading-unloading cycles; (b) avalanche distributions of cyclically loaded crystals for the first and the second cycles; the first cycle is understood as the monotone loading path. Here $\delta_h = \delta = 0.30$, $\delta_g = 0.30$. Adapted with permission from [67]. Copyrighted by American Physical Society.

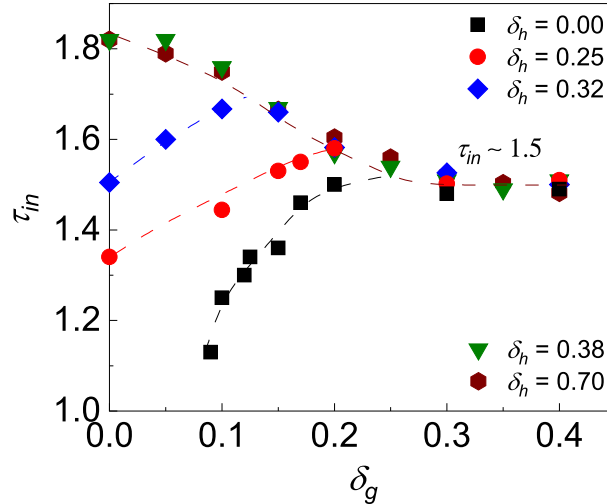


Figure 12. Effect of the “local” disorder δ_g on the (integrated) scaling exponent τ_{in} for the case of cyclic loading. Adapted with permission from [67]. Copyrighted by American Physical Society.

is weak, we recover the after-yield behavior studied above. At stronger “local” disorder, the dependence of the exponent τ_{in} on the “nonlocal” disorder progressively diminishes. Given that the statistics is mostly acquired during hardening-free yield, see Figure 11, one can expect the stress resolved value of the exponent τ to be similar to the aggregate value τ_{in} [139]. In this case the obtained exponent value suggests mean field criticality [137, 138]. In other words, the abundance of “local” disorder apparently trivializes the scaling picture, erasing the non-universality and promoting a universal response of the athermally driven infinite dimensional RFIM dominating the response of amorphous solids [132, 140–142].

However, the overall agreement between our automaton model, which is based on some crude assumptions, and experiments, is incomplete. Thus, in experiments, we encounter distributions of avalanche sizes mixing a power law tail with a *lower* cut-off below which fluctuations are mild.

This wild-to-mild coexistence and its unique signatures, such as the relationship between κ and the wildness W (Figure 5(c)), are not recovered within this oversimplified model. The problem is most probably in the single-slip assumption that prevents the emergence of metastable dislocation patterns. Another shortcoming is that disorder is prescribed as a single-scale field so that, by construction, fluctuations at smaller scales are compromised.

5.2. Mean-field model

A simple mean field model can be used to rationalize at least some elements of the observed bigger picture in terms of macroscopic parameters. In particular, it will allow us to explain the coexistence of mild and wild fluctuations in crystalline plasticity.

Suppose that the stress-resolved evolution of the spatially averaged density of *mobile* dislocations ρ is described by a stochastic kinetic equation [62]

$$\rho^{-1} d\rho/d\gamma = a\rho^{-1} - c + \sqrt{2D}\eta(\gamma), \quad (14)$$

where the local shear strain γ serves as a time-like parameter, $c \geq 0$ characterizes the rate of dislocation immobilization and the temperature-like parameter D represents the intensity of the multiplicative mechanical noise with $\langle \eta(\gamma) \rangle = 0$ and $\langle \eta(\gamma_1)\eta(\gamma_2) \rangle = \delta(\gamma_1 - \gamma_2)$. In view of the constant stress assumption, the route towards yielding in a stress-tuned regime cannot be described in this way, however this model can be used to rationalize the universal dependence of wildness on both material characteristics and sample size.

While the deterministic part of the model (the first two terms on the RHS of (14)) is quite conventional, in this simplified framework the long-ranged stochastic interactions are described through a multiplicative noise. The level of noise D quantifies the intensity of mechanical fluctuations experienced by a meso-volume due to interactions with the rest of the system. A concept of “mechanical temperature” has been also used in the modelling of athermal amorphous plasticity [143]. Considering the Orowan’s relation $d\gamma = \rho b v dt$, and assuming a constant dislocation velocity v under constant stress, we can link the fluctuations of ρ with the experimentally measured strain (or slip X) fluctuations.

The stationary probability distribution in (14) is $p_s(\rho) \sim e^{-a/(D\rho)} \rho^{-\alpha}$ with the exponent $\alpha = 1 + c/D$. This is exactly the same expression as our empirical equation (1) with $\kappa - 1 = c/D$ and $X_0 \sim a/D$ [62, 64]. Consequently, the wildness W is given by expression (3). Therefore, though oversimplified, our mean field model predicts a relationship between the exponent κ and the wildness W , which are linked through the characteristic size X_0 which represents a material constant. We reiterate that the existence of such universal relation between the structure of the power law tail of avalanche distribution and the wildness parameter W is in full agreement with the observed data for a large number of pure materials and alloys (Figure 5(c)).

In the framework of our automaton model we can interpret ρ as the density of mobile dislocations during an avalanche at a given value of the loading γ . We can then write $\rho(\gamma) = n(\gamma)/N^2$, where $n(\gamma)$ is the number of dislocations moved during an avalanche. Our numerical experiments suggest that the avalanche energy E is a disorder independent linear function of the total distance traveled by mobile dislocations during an avalanche \bar{l} and that $\bar{l} \sim n$. Therefore $E \sim \rho$ and we can conclude that the exponent α in the mean field model should be indeed the same as the exponent κ in the automaton model.

For single slip pure nano-crystals with weak disorder, dislocation immobilization can be neglected, so $c/D \ll 1$, and the stochastic evolution of ρ governed by (14) reduces in this case to a geometric Brownian motion with $\alpha \sim 1$. In the automaton model we observe in the low-disorder limit dislocation self-organization, governed exclusively by elastic long-range elastic interactions [33, 50], and recover the same value of the exponent $\kappa \sim 1$. With increasing disorder,

the immobilization rate c should increase leading to a higher value of κ , which is in qualitative agreement with our numerical experiments.

The crossover from D -dominated brittle regimes ($c < D$ with the stochastic term in (14) controlling the dynamics) to c -dominated ductile regimes ($c > D$ with the deterministic term in (14) controlling the dynamics) can be expected where the mechanical agitation is balanced by dislocation self-locking ($c \sim D$). Using the relation $\alpha = \kappa$, we can now link c/D and $R = L/l$. The effective temperature D should depend only weakly on the system size L . It is defined instead by the locking strength of defects, which means that it increases with l . At the same time, it is clear that the rate of dislocation reactions (in particular our parameter c controlling immobilization) increases with L [64]. Therefore, in either very small and/or very weakly disordered samples $c < D$. Conversely, in either bigger or more disordered samples one can expect to reach the ductile phase where $c > D$. We recall that all these trends were observed in our automaton model.

We can go a little further in the interpretation of the model parameters focusing now on the role of the parameter a . In fact, the model has two characteristic densities $\rho_c = a/c$ and $\rho_D = a/D$ or, in other words, two characteristic length scales $l_c = 1/\sqrt{\rho_c}$ and $l_D = 1/\sqrt{\rho_D}$. The scale ratio $r = l_c/l_D = \sqrt{c/D} = \sqrt{\kappa - 1}$ is then the main dimensionless parameter of the mean field model and it should then control the wildness $W = W(\kappa) = W(r)$, see (3). On the other hand, we argued, and showed experimentally (Figure 5(b)) that W is controlled by the ratio $R = L/l$. By comparing the functions $W(r)$ and $W(R)$ we find that $R \sim r^2$ because the relation $\kappa - 1 = c/D \sim L/l = R$ has been verified experimentally [64]. This suggests $c \sim L$ and $D \sim l$, i.e., for a given material, c expresses an external size effect, while D accounts for an internal scale effect [64].

In particular, in HCP pure materials, such as ice or Mg, single-slip plasticity and the absence of forest hardening implies a negligible immobilization of dislocation pairs, i.e. a small c value. In addition, for the reasons already discussed in Section 2.4, the pinning strength τ_{pin} is small, which we can now interpret as a large mechanical temperature $D \sim l \sim 1/\tau_{\text{pin}}$ [64]. This combination gives a small κ , close to 1, and a large wildness, as observed (Figure 5(c)). On the reverse, for hardened and/or alloyed large FCC metallic samples, we expect a small value of D as well as an enhanced immobilization term resulting from the ubiquity of locks and junctions. All this means large κ and a small W .

6. Conclusions

Dynamical fluctuations have been for a long time overlooked in the studies of crystalline plasticity. An implicit assumption has been that such fluctuations average out when the phenomenon is considered on “large enough” spatial and temporal scales. The situation has changed over recent years driven by the efforts to progressively miniaturize various mechanical devices. As a result, the mechanical properties of metallic materials at micro- to nano-scales have become a major concern in the material science community. If the classical metallurgical practices have been developed to optimize strength, formability, and resistance to fatigue for samples at macroscopic scales, similar questions have arisen in microscopic metallurgy dealing with sub- μm scales.

In this review we have presented a highly subjective outlook on plastic fluctuations in pure materials and alloys with quenched disorder. It reveals a rich and intricate landscape of behaviors and scaling properties that defies conventional phenomenological approaches and call for a paradigm change. We are witnessing an opening of materials science and metallurgy to the powerful methods and techniques of nonequilibrium statistical physics.

In HCP materials, characterized by a low lattice friction and a strong plastic anisotropy, dislocation avalanches are detectable even on macroscopic bulk scales. They are power-law distributed in size and energy which suggests critical dynamics, reminiscent of developed turbulence. However, at macroscopic scales, such wild fluctuations are nearly undetectable in most of

the situations of interest to classical metallurgy. This is particularly true for bulk FCC and BCC metals and their alloys, especially once strain hardening takes place. The small relative scale of plastic fluctuations explains the lack of interest to this subject until recent times when ultra-small structures started to enter industrial applications.

The “smaller is stronger” size effect, emerging at these scales, appears beneficial at first glance. However, it is corrupted by wild plastic fluctuations, which in the case of sub-micron samples can occasionally reach the system size and produce a brittle-like response. In other words, despite the extremely high strength achievable at ultra-small scales, the corresponding plastic flows turned out to be uncontrollable due to the stochastic nature of strain bursts reminiscent of macroscopic earthquakes. The disastrous dislocation avalanches not only poison the forming processes but also compromise the load-carrying capacity in various engineering/industrial processes dealing with sub- μm parts, including nanoimprint lithography [118] and shaping of MEMS [37]. An urgent challenge facing today’s metallurgy at sub- μm scales is, therefore, to reduce the “wildness” of the associated fluctuations, while keeping or improving other properties, such as strength.

In this review we focused on the important fact that the transition from a mild to a wild plasticity is controlled by a dimensionless ratio of length scales which we denoted by $R = L/l$, where L and l are external and internal scales, respectively. In FCC pure materials, the internal scale l can be linked to a dislocation mean free path, hence to dislocation patterning and hardening. Instead, lattice friction may play a significant role in shaping the value of l in BCC materials at low temperatures. Thinking in terms of R also suggests that plastic intermittency can be reduced or shifted towards smaller system sizes by introducing quenched disorder through alloying and other similar means. Our experimental results fully support the feasibility of such a “dirtier is milder” metallurgical strategy.

While these first steps in harnessing plastic fluctuations at ultra-small scales have been successful, many key challenges persist. Some of them are listed below:

(i) In case of HCP materials, the possibility to tame wild fluctuations at bulk scales, by introducing tailored disorder, remains to be explored.

(ii) Finding the effect of lattice friction and thermally activated processes below the athermal temperature on plastic fluctuations in BCC materials requires a systematic analysis.

(iii) In weakly disordered and dislocation-free or strongly starved FCC crystals, we identified a transition from a spin-glass type marginality to a spinodal stress-tuned criticality. Both regimes are associated with deleterious system-spanning instabilities and a brittle-like behavior. It is still unclear how such brittleness can be controlled without introducing stronger doping.

(iv) In this review, we did not discuss the structure of individual dislocation avalanches—how they initially intensify and then fade away—the so-called avalanche shape [144], and in fact this topic has been mostly avoided in plasticity [145]. It deserves much more attention, as the avalanche shape can carry a strong signature of the underlying crystal symmetry.

(v) At small scales, stochasticity results in an increasing variability of “global” mechanical characteristics like strength [39, 146] and hardening coefficient (e.g. Figure 7). This large scatter is a deleterious effect and this problem recently emerged most clearly in the context of nano-indentation [147]. As in fracture of disordered materials (e.g. [148]), the analysis of finite-size effects on strength *variability* is then of crucial importance.

(vi) The conceptual stochastic models of plasticity, discussed in Section 5, remain too schematic to adequately account for the geometry of real systems and the complexity of the associated loading protocols. In other words, realistic problems are still outside the realm of numerical modeling by stochastic differential equations. DDD simulations have been extensively used to model the associated systems but the predictive power of this approach remains limited because of the ever-increasing number of ad-hoc rules required for its implementation. An al-

ternative may be found in embedding of stochastic rheological closure relations within (so far) deterministic finite-element (FE) codes.

Acknowledgements

We would like to thank David Rodney for highly valuable comments and suggestions. This work was supported by French-Chinese ANR-NSFC grant (ANR-19-CE08-0010-01 and 51761135031). PZ acknowledges additional support from China Scholarship Council and China Postdoctoral Science Foundation (grant 2019M653595).

References

- [1] R. Becker, E. Orowan, "Sudden expansion of zinc crystals", *Z. Phys.* **79** (1932), p. 566-572.
- [2] J. Weiss, J.-R. Grasso, "Acoustic emission in single crystals of ice", *J. Phys. Chem. B* **101** (1997), no. 32, p. 6113-6117.
- [3] M.-C. Miguel, A. Vespignani, S. Zapperi, J. Weiss, J.-R. Grasso, "Intermittent dislocation flow in viscoplastic deformation", *Nature* **410** (2001), no. 6829, p. 667-671.
- [4] D. M. Dimiduk, C. Woodward, R. LeSar, M. D. Uchic, "Scale-free intermittent flow in crystal plasticity", *Science* **312** (2006), no. 5777, p. 1188-1190.
- [5] N. Friedman, A. T. Jennings, G. Tsekenis, J.-Y. Kim, M. Tao, J. T. Uhl, J. R. Greer, K. A. Dahmen, "Statistics of dislocation slip avalanches in nanosized single crystals show tuned critical behavior predicted by a simple mean field model", *Phys. Rev. Lett.* **109** (2012), no. 9, article no. 095507.
- [6] E. Orowan, "Zur kristallplastizität. I", *Z. Phys.* **89** (1934), no. 9-10, p. 605-613.
- [7] E. Orowan, "Zur kristallplastizität. II", *Z. Phys.* **89** (1934), no. 9-10, p. 614-633.
- [8] E. Orowan, "Zur kristallplastizität. III", *Z. Phys.* **89** (1934), no. 9-10, p. 634-659.
- [9] M. Polanyi, "Über eine Art Gitterstörung, die einen Kristall plastisch machen könnte", *Z. Phys.* **89** (1934), no. 9-10, p. 660-664.
- [10] G. I. Taylor, "The mechanism of plastic deformation of crystals. Part I.—Theoretical", *Proc. R. Soc. Lond. A* **145** (1934), no. 855, p. 362-387.
- [11] A. Timpe, "Probleme der Spannungsverteilung in ebenen Systemen einfach gelöst mit Hilfe der Airyschen Function", *Z. Math. Phys.* **52** (1905), p. 348-383.
- [12] V. Volterra, "Sur l'équilibre des corps élastiques multiplement connexes", *Ann. Sci. Éc. Norm. Supér.* **24** (1907), p. 401-517.
- [13] J. Hirth, "A brief history of dislocation theory", *Metall. Trans. A* **16** (1985), no. 12, p. 2085-2090.
- [14] J. Savage, "Dislocations in seismology", *Dislocations Solids* **3** (1980), p. 251-339.
- [15] A. Garroni, S. Müller, "Γ-limit of a phase-field model of dislocations", *SIAM J. Math. Anal.* **36** (2005), no. 6, p. 1943-1964.
- [16] M. Ariza, M. Ortiz, "Discrete crystal elasticity and discrete dislocations in crystals", *Arch. Ration. Mech. Anal.* **178** (2005), no. 2, p. 149-226.
- [17] J. Nye, "Some geometrical relations in dislocated crystals", *Acta Metall.* **1** (1953), no. 2, p. 153-162.
- [18] E. Kröner, "Allgemeine kontinuumstheorie der versetzungen und eigenspannungen", *Arch. Ration. Mech. Anal.* **4** (1959), no. 1, article no. 273.
- [19] J. Hutchinson, N. Fleck, "Strain gradient plasticity", *Adv. Appl. Mech.* **33** (1997), p. 295-361.
- [20] A. Acharya, J. Bassani, "Lattice incompatibility and a gradient theory of crystal plasticity", *J. Mech. Phys. Solids* **48** (2000), no. 8, p. 1565-1595.
- [21] A. Acharya, "A model of crystal plasticity based on the theory of continuously distributed dislocations", *J. Mech. Phys. Solids* **49** (2001), no. 4, p. 761-784.
- [22] C. Fressengeas, V. Taupin, L. Capolungo, "An elasto-plastic theory of dislocation and disclination fields", *Int. J. Solids Struct.* **48** (2011), no. 25-26, p. 3499-3509.
- [23] P.-L. Valdenaire, Y. Le Bouar, B. Appolaire, A. Finel, "Density-based crystal plasticity: From the discrete to the continuum", *Phys. Rev. B* **93** (2016), no. 21, article no. 214111.
- [24] L. P. Kubin, G. Canova, M. Condat, B. Devincere, V. Pontikis, Y. Bréchet, "Dislocation microstructures and plastic flow: A 3D simulation", in *Solid State Phenomena*, vol. 23, Trans. Tech. Publ., 1992, p. 455-472.
- [25] L. Kubin, *Dislocations, Mesoscale Simulations and Plastic Flow*, vol. 5, Oxford University Press, 2013.
- [26] D. Rodney, "Molecular dynamics simulation of screw dislocations interacting with interstitial frank loops in a model FCC crystal", *Acta Mater.* **52** (2004), no. 3, p. 607-614.
- [27] L. A. Zepeda-Ruiz, A. Stukowski, T. Oppelstrup, V. V. Bulatov, "Probing the limits of metal plasticity with molecular dynamics simulations", *Nature* **550** (2017), no. 7677, p. 492-495.

- [28] R. Madec, B. Devincre, L. Kubin, "Simulation of dislocation patterns in multislip", *Scr. Mater.* **47** (2002), no. 10, p. 689-695.
- [29] L. Kubin, C. Fressengeas, G. Ananthakrishna, "Collective behaviour of dislocations in plasticity", *Dislocations in Solids* **11** (2002), p. 101-192.
- [30] P. Hähner, K. Bay, M. Zaiser, "Fractal dislocation patterning during plastic deformation", *Phys. Rev. Lett.* **81** (1998), no. 12, p. 2470-2473.
- [31] C. Laird, P. Charsley, H. Mughrabi, "Low energy dislocation structures produced by cyclic deformation", *Mater. Sci. Eng.* **81** (1986), p. 433-450.
- [32] M. Sauzay, L. P. Kubin, "Scaling laws for dislocation microstructures in monotonic and cyclic deformation of fcc metals", *Prog. Mater. Sci.* **56** (2011), no. 6, p. 725-784.
- [33] J. Weiss, "Ice: The paradigm of wild plasticity", *Philos. Trans. R. Soc. Lond. A* **377** (2019), no. 2146, article no. 20180260.
- [34] S. Brinckmann, J.-Y. Kim, J. R. Greer, "Fundamental differences in mechanical behavior between two types of crystals at the nanoscale", *Phys. Rev. Lett.* **100** (2008), no. 15, article no. 155502.
- [35] K. Ng, A. Ngan, "Stochastic nature of plasticity of aluminum micro-pillars", *Acta Mater.* **56** (2008), no. 8, p. 1712-1720.
- [36] F. F. Csikor, C. Motz, D. Weygand, M. Zaiser, S. Zapperi, "Dislocation avalanches strain bursts and the problem of plastic forming at the micrometer scale", *Science* **318** (2007), no. 5848, p. 251-254.
- [37] T. Hu, L. Jiang, A. K. Mukherjee, J. M. Schoenung, E. J. Lavner, "Strategies to approach stabilized plasticity in metals with diminutive volume: A brief review", *Crystals* **6** (2016), no. 8, article no. 92.
- [38] M. Zaiser, P. Moretti, "Fluctuation phenomena in crystal plasticity—a continuum model", *J. Stat. Mech.: Theory Exp.* **2005** (2005), no. 08, article no. P08004.
- [39] M. Zaiser, "Statistical aspects of microplasticity: Experiments, discrete dislocation simulations and stochastic continuum models", *J. Mech. Behav. Mater.* **22** (2013), no. 3–4, p. 89-100.
- [40] S. Xia, A. El-Azab, "Computational modelling of mesoscale dislocation patterning and plastic deformation of single crystals", *Modell. Simul. Mater. Sci. Eng.* **23** (2015), no. 5, article no. 055009.
- [41] M. Monavari, M. Zaiser, "Annihilation and sources in continuum dislocation dynamics", *Mater. Theory* **2** (2018), no. 1, article no. 3.
- [42] M. Lebyodkin, Y. Brechet, Y. Estrin, L. Kubin, "Statistics of the catastrophic slip events in the Portevin–Le Châtelier effect", *Phys. Rev. Lett.* **74** (1995), no. 23, p. 4758.
- [43] G. Ananthakrishna, S. Noronha, C. Fressengeas, L. Kubin, "Crossover from chaotic to self-organized critical dynamics in jerky flow of single crystals", *Phys. Rev. E* **60** (1999), no. 5, p. 5455-5462.
- [44] M. Bharathi, M. Lebyodkin, G. Ananthakrishna, C. Fressengeas, L. Kubin, "The hidden order behind jerky flow", *Acta Mater.* **50** (2002), no. 11, p. 2813-2824.
- [45] G. Ananthakrishna, "Current theoretical approaches to collective behavior of dislocations", *Phys. Rep.* **440** (2007), no. 4–6, p. 113-259.
- [46] Y. R. Efendiev, L. Truskinovsky, "Thermalization of a driven bi-stable FPU chain", *Contin. Mech. Thermodyn.* **22** (2010), no. 6, p. 679-698.
- [47] V. Berdichevsky, "Beyond classical thermodynamics: Dislocation-mediated plasticity", *J. Mech. Phys. Solids* **129** (2019), p. 83-118.
- [48] J. Langer, E. Bouchbinder, T. Lookman, "Thermodynamic theory of dislocation-mediated plasticity", *Acta Mater.* **58** (2010), no. 10, p. 3718-3732.
- [49] J. Langer, "Statistical thermodynamics of dislocations in solids", <https://arxiv.org/abs/2003.03209>, 2020.
- [50] P. D. Ispánovity, L. Laurson, M. Zaiser, I. Groma, S. Zapperi, M. J. Alava, "Avalanches in 2D dislocation systems: Plastic yielding is not depinning", *Phys. Rev. Lett.* **112** (2014), no. 23, article no. 235501.
- [51] H. Song, D. Dimiduk, S. Papanikolaou, "Universality class of nanocrystal plasticity: Localization and self-organization in discrete dislocation dynamics", *Phys. Rev. Lett.* **122** (2019), no. 17, article no. 178001.
- [52] M. Zaiser, "Scale invariance in plastic flow of crystalline solids", *Adv. Phys.* **55** (2006), no. 1–2, p. 185-245.
- [53] M. D. Uchic, P. A. Shade, D. M. Dimiduk, "Plasticity of micrometer-scale single crystals in compression", *Annu. Rev. Mater. Res.* **39** (2009), p. 361-386.
- [54] J. R. Greer, J. T. M. De Hosson, "Plasticity in small-sized metallic systems: Intrinsic versus extrinsic size effect", *Prog. Mater. Sci.* **56** (2011), no. 6, p. 654-724.
- [55] S. Papanikolaou, Y. Cui, N. Ghoniem, "Avalanches and plastic flow in crystal plasticity: An overview", *Model. Simul. Mat. Sci. Eng.* **26** (2017), no. 1, article no. 013001.
- [56] R. Maass, P. Derlet, "Micro-plasticity and recent insights from intermittent and small-scale plasticity", *Acta Mater.* **143** (2018), p. 338-363.
- [57] Y. Cui, N. Ghoniem, "Spatio-temporal plastic instabilities at the nano/micro scale", *J. Micromech. Mol. Phys.* **3** (2018), no. 03n04, article no. 1840006.
- [58] J. P. Sethna, M. K. Bierbaum, K. A. Dahmen, C. P. Goodrich, J. R. Greer, L. X. Hayden, J. P. Kent-Dobias, E. D. Lee, D. B.

- Liarte, X. Ni *et al.*, “Deformation of crystals: Connections with statistical physics”, *Annu. Rev. Mater. Res.* **47** (2017), p. 217-246.
- [59] I. Ovid’Ko, R. Valiev, Y. Zhu, “Review on superior strength and enhanced ductility of metallic nanomaterials”, *Prog. Mater. Sci.* **94** (2018), p. 462-540.
- [60] G. Dehm, B. N. Jaya, R. Raghavan, C. Kirchlechner, “Overview on micro-and nanomechanical testing: New insights in interface plasticity and fracture at small length scales”, *Acta Mater.* **142** (2018), p. 248-282.
- [61] I. Groma, “Statistical theory of dislocation”, in *Mesoscale Models* (S. Mesarovic, S. Forest, H. Zbib, eds.), CISM International Centre for Mechanical Sciences (Courses and Lectures), vol. 587, Springer, 2019, p. 87-139.
- [62] J. Weiss, W. B. Rhouma, T. Richeton, S. Dechanel, F. Louchet, L. Truskinovsky, “From mild to wild fluctuations in crystal plasticity”, *Phys. Rev. Lett.* **114** (2015), no. 10, article no. 105504.
- [63] S. Papanikolaou, D. M. Dimiduk, W. Choi, J. P. Sethna, M. D. Uchic, C. F. Woodward, S. Zapperi, “Quasi-periodic events in crystal plasticity and the self-organized avalanche oscillator”, *Nature* **490** (2012), no. 7421, p. 517-521.
- [64] P. Zhang, O. U. Salman, J.-Y. Zhang, G. Liu, J. Weiss, L. Truskinovsky, J. Sun, “Taming intermittent plasticity at small scales”, *Acta Mater.* **128** (2017), p. 351-364.
- [65] M. Zaiser, N. Nikitas, “Slip avalanches in crystal plasticity: Scaling of the avalanche cut-off”, *J. Stat. Mech.: Theory Exp.* **2007** (2007), no. 04, article no. P04013.
- [66] J. Weiss, W. B. Rhouma, S. Dechanel, L. Truskinovsky, “Plastic intermittency during cyclic loading: From dislocation patterning to microcrack initiation”, *Phys. Rev. Mater.* **3** (2019), no. 2, article no. 023603.
- [67] P. Zhang, O. Salman, J. Weiss, L. Truskinovsky, “Variety of scaling behaviors in nanocrystalline plasticity”, *Phys. Rev. E* **102** (2020), article no. 023006.
- [68] P. Zhang, J.-J. Bian, J.-Y. Zhang, G. Liu, J. Weiss, J. Sun, “Plate-like precipitate effects on plasticity of Al-Cu alloys at micrometer to sub-micrometer scales”, *Mater. Design* **188** (2020), article no. 108444.
- [69] G. l’Hôte, S. Cazottes, J. Lachambre, M. Montagnat, P. Courtois, J. Weiss, S. Dechanel, “Dislocation dynamics during cyclic loading in copper single crystal”, *Materialia* **8** (2019), article no. 100501.
- [70] O. U. Salman, L. Truskinovsky, “Minimal integer automaton behind crystal plasticity”, *Phys. Rev. Lett.* **106** (2011), no. 17, article no. 175503.
- [71] R. Tinder, J. Trzil, “Millimicroplastic burst phenomena in zinc monocrystals”, *Acta Metall.* **21** (1973), no. 7, p. 975-989.
- [72] R. Fisher, J. Lally, “Microplasticity detected by an acoustic technique”, *Can. J. Phys.* **45** (1967), no. 2, p. 1147-1159.
- [73] D. R. James, S. H. Carpenter, “Relationship between acoustic emission and dislocation kinetics in crystalline solids”, *J. Appl. Phys.* **42** (1971), no. 12, p. 4685-4697.
- [74] T. Imanaka, K. Sano, M. Shimizu, “Dislocation attenuation and acoustic emission during deformation in copper single crystals”, *Cryst. Lattice Defects* **4** (1973), no. 1, p. 57-64.
- [75] N. Kiesewetter, P. Schiller, “The acoustic emission from moving dislocations in aluminium”, *Phys. Status Solidi (a)* **38** (1976), no. 2, p. 569-576.
- [76] P. D. Rouby, P. Fleischmann, C. Duvergier, “Un modèle de sources d’émission acoustique pour l’analyse de l’émission continue et de l’émission par sèves I. Analyse théorique”, *Philos. Mag. A* **47** (1983), no. 5, p. 671-687.
- [77] P. Duval, M. Ashby, I. Anderman, “Rate-controlling processes in the creep of polycrystalline ice”, *J. Phys. Chem.* **87** (1983), no. 21, p. 4066-4074.
- [78] J. T. Uhl, S. Pathak, D. Schorlemmer, X. Liu, R. Swindeman, B. A. Brinkman, M. LeBlanc, G. Tsekenis, N. Friedman, R. Behringer *et al.*, “Universal quake statistics: From compressed nanocrystals to earthquakes”, *Sci. Rep.* **5** (2015), article no. 16493.
- [79] E. K. Salje, K. A. Dahmen, “Crackling noise in disordered materials”, *Annu. Rev. Condens. Matter Phys.* **5** (2014), p. 233-254.
- [80] J. Weiss, M. C. Miguel, “Dislocation avalanche correlations”, *Mater. Sci. Eng. A* **387** (2004), p. 292-296.
- [81] J. Weiss, D. Marsan, “Three-dimensional mapping of dislocation avalanches: Clustering and space/time coupling”, *Science* **299** (2003), no. 5603, p. 89-92.
- [82] T. Richeton, P. Dobron, F. Chmelik, J. Weiss, F. Louchet, “On the critical character of plasticity in metallic single crystals”, *Mater. Sci. Eng. A* **424** (2006), no. 1-2, p. 190-195.
- [83] J. Weiss, T. Richeton, F. Louchet, F. Chmelik, P. Dobron, D. Entemeyer, M. Lebyodkin, T. Lebedkina, C. Fressengeas, R. J. McDonald, “Evidence for universal intermittent crystal plasticity from acoustic emission and high-resolution extensometry experiments”, *Phys. Rev. B* **76** (2007), no. 22, article no. 224110.
- [84] Y. Chen, B. Gou, W. Fu, C. Chen, X. Ding, J. Sun, E. K. Salje, “Fine structures of acoustic emission spectra: How to separate dislocation movements and entanglements in 316L stainless steel”, *Appl. Phys. Lett.* **117** (2020), no. 26, article no. 262901.
- [85] T. Richeton, J. Weiss, F. Louchet, “Breakdown of avalanche critical behaviour in polycrystalline plasticity”, *Nat. Mater.* **4** (2005), no. 6, p. 465-469.
- [86] T. Niiyama, T. Shimokawa, “Barrier effect of grain boundaries on the avalanche propagation of polycrystalline plasticity”, *Phys. Rev. B* **94** (2016), no. 14, article no. 140102.

- [87] T. Richeton, J. Weiss, F. Louchet, “Dislocation avalanches: Role of temperature, grain size and strain hardening”, *Acta Mater.* **53** (2005), no. 16, p. 4463-4471.
- [88] J. Schiøtz, K. W. Jacobsen, “A maximum in the strength of nanocrystalline copper”, *Science* **301** (2003), no. 5638, p. 1357-1359.
- [89] F. Louchet, J. Weiss, T. Richeton, “Hall–Petch law revisited in terms of collective dislocation dynamics”, *Phys. Rev. Lett.* **97** (2006), no. 7, article no. 075504.
- [90] M. D. Uchic, D. M. Dimiduk, J. N. Florando, W. D. Nix, “Sample dimensions influence strength and crystal plasticity”, *Science* **305** (2004), no. 5686, p. 986-989.
- [91] G. Richter, K. Hillerich, D. S. Gianola, R. Monig, O. Kraft, C. A. Volkert, “Ultrahigh strength single crystalline nanowhiskers grown by physical vapor deposition”, *Nano Lett.* **9** (2009), no. 8, p. 3048-3052.
- [92] A. Sharma, J. Hickman, N. Gazit, E. Rabkin, Y. Mishin, “Nickel nanoparticles set a new record of strength”, *Nat. Commun.* **9** (2018), no. 1, article no. 4102.
- [93] D. Mordehai, O. David, R. Kositski, “Nucleation-controlled plasticity of metallic nanowires and nanoparticles”, *Adv. Mater.* **30** (2018), no. 41, article no. 1706710.
- [94] D. Dunstan, A. Bushby, “The scaling exponent in the size effect of small scale plastic deformation”, *Int. J. Plast.* **40** (2013), p. 152-162.
- [95] A. Schneider, D. Kaufmann, B. Clark, C. Frick, P. Gruber, R. Mönig, O. Kraft, E. Arzt, “Correlation between critical temperature and strength of small-scale bcc pillars”, *Phys. Rev. Lett.* **103** (2009), no. 10, article no. 105501.
- [96] T. A. Parthasarathy, S. I. Rao, D. M. Dimiduk, M. D. Uchic, D. R. Trinkle, “Contribution to size effect of yield strength from the stochastics of dislocation source lengths in finite samples”, *Scr. Mater.* **56** (2007), no. 4, p. 313-316.
- [97] J. R. Greer, W. D. Nix, “Nanoscale gold pillars strengthened through dislocation starvation”, *Phys. Rev. B* **73** (2006), no. 24, article no. 245410.
- [98] M. Zaiser, J. Schwerdtfeger, A. Schneider, C. Frick, B. G. Clark, P. Gruber, E. Arzt, “Strain bursts in plastically deforming molybdenum micro- and nanopillars”, *Philos. Mag. A* **88** (2008), no. 30–32, p. 3861-3874.
- [99] A. Lehtinen, G. Costantini, M. J. Alava, S. Zapperi, L. Laurson, “Glassy features of crystal plasticity”, *Phys. Rev. B* **94** (2016), no. 6, article no. 064101.
- [100] R. Maaß, P. M. Derlet, J. R. Greer, “Small-scale plasticity: Insights into dislocation avalanche velocities”, *Scr. Mater.* **69** (2013), no. 8, p. 586-589.
- [101] A. Clauset, C. R. Shalizi, M. E. Newman, “Power-law distributions in empirical data”, *SIAM Rev.* **51** (2009), no. 4, p. 661-703.
- [102] D. Sornette, G. Ouillon, “Dragon-kings: Mechanisms, statistical methods and empirical evidence”, *Eur. Phys. J.: Spec. Top.* **205** (2012), no. 1.
- [103] D. Mordehai, S.-W. Lee, B. Backes, D. J. Srolovitz, W. D. Nix, E. Rabkin, “Size effect in compression of single-crystal gold microparticles”, *Acta Mater.* **59** (2011), no. 13, p. 5202-5215.
- [104] J. R. Rice, R. Thomson, “Ductile versus brittle behaviour of crystals”, *Philos. Mag. A* **29** (1974), no. 1, p. 73-97.
- [105] P. Gumbsch, J. Riedle, A. Hartmaier, H. F. Fischmeister, “Controlling factors for the brittle-to-ductile transition in tungsten single crystals”, *Science* **282** (1998), no. 5392, p. 1293-1295.
- [106] B. D. Wirth, “How does radiation damage materials?”, *Science* **318** (2007), no. 5852, p. 923-924.
- [107] D. Kiener, C. Motz, M. Rester, M. Jenko, G. Dehm, “FIB damage of Cu and possible consequences for miniaturized mechanical tests”, *Mater. Sci. Eng. A* **459** (2007), no. 1–2, p. 262-272.
- [108] S. Lee, J. Jeong, Y. Kim, S. M. Han, D. Kiener, S. H. Oh, “FIB-induced dislocations in Al submicron pillars: Annihilation by thermal annealing and effects on deformation behavior”, *Acta Mater.* **110** (2016), p. 283-294.
- [109] J. Weiss, F. Louchet, “Seismology of plastic deformation”, *Scr. Mater.* **54** (2006), no. 5, p. 747-751.
- [110] D. Rodney, L. Ventelon, E. Clouet, L. Pizzagalli, F. Willaime, “*Ab initio* modeling of dislocation core properties in metals and semiconductors”, *Acta Mater.* **124** (2017), p. 633-659.
- [111] O. T. Abad, J. M. Wheeler, J. Michler, A. S. Schneider, E. Arzt, “Temperature-dependent size effects on the strength of Ta and W micropillars”, *Acta Mater.* **103** (2016), p. 483-494.
- [112] Y. Cui, G. Po, P. Srivastava, K. Jiang, V. Gupta, N. Ghoniem, “The role of slow screw dislocations in controlling fast strain avalanche dynamics in body-centered cubic metals”, *Int. J. Plast.* **124** (2020), p. 117-132.
- [113] G. Sparks, Y. Cui, G. Po, Q. Rizzardi, J. Marian, R. Maaß, “Avalanche statistics and the intermittent-to-smooth transition in microplasticity”, *Phys. Rev. Mater.* **3** (2019), no. 8, article no. 080601.
- [114] Y. Cui, G. Po, N. Ghoniem, “Temperature insensitivity of the flow stress in body-centered cubic micropillar crystals”, *Acta Mater.* **108** (2016), p. 128-137.
- [115] A. Keh, S. Weissmann, “Deformation substructure in body-centered cubic metals”, in *Electron Microscopy and Strength of Crystals*, Interscience, New York, 1963, p. 231-300.
- [116] M. Zaiser, S. Sandfeld, “Scaling properties of dislocation simulations in the similitude regime”, *Model. Simul. Mat. Sci. Eng.* **22** (2014), no. 6, article no. 065012.
- [117] J. D. Verhoeven, A. Pendray, W. Dauksch, “The key role of impurities in ancient Damascus steel blades”, *JOM* **50** (1998), no. 9, p. 58-64.

- [118] H. Gao, Y. Hu, Y. Xuan, J. Li, Y. Yang, R. V. Martinez, C. Li, J. Luo, M. Qi, G. J. Cheng, "Large-scale nanoshaping of ultrasmooth 3D crystalline metallic structures", *Science* **346** (2014), no. 6215, p. 1352-1356.
- [119] R. Gu, A. Ngan, "Size effect on the deformation behavior of duralumin micropillars", *Scr. Mater.* **68** (2013), no. 11, p. 861-864.
- [120] B. Girault, A. S. Schneider, C. P. Frick, E. Arzt, "Strength effects in micropillars of a dispersion strengthened superalloy", *Adv. Eng. Mater.* **12** (2010), no. 5, p. 385-388.
- [121] Y. Pan, H. Wu, X. Wang, Q. Sun, L. Xiao, X. Ding, J. Sun, E. K. Salje, "Rotatable precipitates change the scale-free to scale dependent statistics in compressed Ti nano-pillars", *Sci. Rep.* **9** (2019), no. 1, article no. 3778.
- [122] D. Bacon, V. Vitek, "Atomic-scale modeling of dislocations and related properties in the hexagonal-close-packed metals", *Metall. Mater. Trans. A* **33** (2002), no. 3, p. 721-733.
- [123] E. Clouet, D. Caillard, N. Chaari, F. Onimus, D. Rodney, "Dislocation locking versus easy glide in titanium and zirconium", *Nat. Mater.* **14** (2015), no. 9, p. 931-936.
- [124] J. A. El-Awady, "Unravelling the physics of size-dependent dislocation-mediated plasticity", *Nat. Commun.* **6** (2015), no. 1, article no. 5926.
- [125] J. Alcalá, J. Očenášek, K. Nowag, D. Esqué-de los Ojos, R. Ghisleni, J. Michler, "Strain hardening and dislocation avalanches in micrometer-sized dimensions", *Acta Mater.* **91** (2015), p. 255-266.
- [126] T. J. Flanagan, O. Kovalenko, E. Rabkin, S.-W. Lee, "The effect of defects on strength of gold microparticles", *Scr. Mater.* **171** (2019), p. 83-86.
- [127] O. U. Salman, L. Truskinovsky, "On the critical nature of plastic flow: One and two dimensional models", *Int. J. Eng. Sci.* **59** (2012), p. 219-254.
- [128] R. Baggio, E. Arbib, P. Biscari, S. Conti, L. Truskinovsky, G. Zanzotto, O. Salman, "Landau-type theory of planar crystal plasticity", *Phys. Rev. Lett.* **123** (2019), no. 20, article no. 205501.
- [129] G. Puglisi, L. Truskinovsky, "Thermodynamics of rate-independent plasticity", *J. Mech. Phys. Solids* **53** (2005), no. 3, p. 655-679.
- [130] G. Picard, A. Ajdari, F. Lequeux, L. Bocquet, "Elastic consequences of a single plastic event: A step towards the microscopic modeling of the flow of yield stress fluids", *Eur. Phys. J. E* **15** (2004), no. 4, p. 371-381.
- [131] B. Tyukodi, S. Patinet, S. Roux, D. Vandembroucq, "From depinning transition to plastic yielding of amorphous media: A soft-modes perspective", *Phys. Rev. E* **93** (2016), no. 6, article no. 063005.
- [132] M. Ozawa, L. Berthier, G. Biroli, A. Rosso, G. Tarjus, "Random critical point separates brittle and ductile yielding transitions in amorphous materials", *Proc. Natl Acad. Sci. USA* **115** (2018), no. 26, p. 6656-6661.
- [133] S. Franz, S. Spigler, "Mean-field avalanches in jammed spheres", *Phys. Rev. E* **95** (2017), no. 2, article no. 022139.
- [134] K. A. Dahmen, Y. Ben-Zion, J. T. Uhl, "Micromechanical model for deformation in solids with universal predictions for stress-strain curves and slip avalanches", *Phys. Rev. Lett.* **102** (2009), no. 17, article no. 175501.
- [135] M. Popović, T. W. de Geus, M. Wyart, "Elastoplastic description of sudden failure in athermal amorphous materials during quasistatic loading", *Phys. Rev. E* **98** (2018), no. 4, article no. 040901.
- [136] S. Suresh, *Fatigue of Materials*, Cambridge University Press, 1998.
- [137] K. Dahmen, J. P. Sethna, "Hysteresis, avalanches, and disorder-induced critical scaling: A renormalization-group approach", *Phys. Rev. B* **53** (1996), no. 22, p. 14872-14905.
- [138] H. B. da Rocha, L. Truskinovsky, "Rigidity-controlled crossover: From spinodal to critical failure", *Phys. Rev. Lett.* **124** (2020), no. 1, article no. 015501.
- [139] G. Durin, S. Zapperi, "The role of stationarity in magnetic crackling noise", *J. Stat. Mech.: Theory Exp.* **2006** (2006), no. 01, article no. P01002.
- [140] M. Ozawa, L. Berthier, G. Biroli, G. Tarjus, "Role of fluctuations in the yielding transition of two-dimensional glasses", *Phys. Rev. Res.* **2** (2020), no. 2, article no. 023203.
- [141] H. Bhaumik, G. Foffi, S. Sastry, "The role of annealing in determining the yielding behavior of glasses under cyclic shear deformation", <https://arxiv.org/abs/1911.12957>, 2019.
- [142] S. Franz, J. Rocchi, "Large deviations of glassy effective potentials", *J. Phys. A: Math. Theor.* **53** (2020), article no. 485002.
- [143] A. Nicolas, K. Martens, J.-L. Barrat, "Rheology of athermal amorphous solids: Revisiting simplified scenarios and the concept of mechanical noise temperature", *Europhys. Lett.* **107** (2014), no. 4, article no. 44003.
- [144] S. Papanikolaou, F. Bohn, R. L. Sommer, G. Durin, S. Zapperi, J. P. Sethna, "Universality beyond power laws and the average avalanche shape", *Nat. Phys.* **7** (2011), no. 4, p. 316-320.
- [145] G. Sparks, R. Maass, "Shapes and velocity relaxation of dislocation avalanches in Au and Nb microcrystals", *Acta Mater.* **152** (2018), p. 86-95.
- [146] A. Rinaldi, P. Peralta, C. Friesen, K. Sieradzki, "Sample-size effects in the yield behavior of nanocrystalline nickel", *Acta Mater.* **56** (2008), no. 3, p. 511-517.
- [147] P. Derlet, R. Maass, "The stress statistics of the first pop-in or discrete plastic event in crystal plasticity", *J. Appl. Phys.* **120** (2016), no. 22, article no. 225101.

- [148] J. Weiss, L. Girard, F. Gimbert, D. Amitrano, D. Vandembroucq, “(Finite) statistical size effects on compressive strength”, *Proc. Natl Acad. Sci. USA* **111** (2014), no. 17, p. 6231-6236.